Syntheses and Properties of Heterobimetallic Ligand-Bridged Ruthenium(II)/Rhenium(I) Complexes and Their Monometallic Congeners

Benjamin J. Coe,*[,†] Emma C. Fitzgerald,[†] Madeleine Helliwell,[†] Bruce S. Brunschwig,[‡] Anthony G. Fitch,[‡] James A. Harris,[‡] Simon J. Coles,[§] Peter N. Horton,[§] and Michael B. Hursthouse[§]

School of Chemistry, University of Manchester, Oxford Road, Manchester M13 9PL, U.K., Molecular Materials Research Center, Beckman Institute, MC 139-74, California Institute of Technology, 1200 East California Boulevard, Pasadena, California 91125, and EPSRC National Crystallography Service, School of Chemistry, University of Southampton, Highfield, Southampton SO17 1BJ, U.K.

Received February 6, 2008

We have prepared three new heterobimetallic complexes containing electron-donating *trans*-$\{Ru^{II}Cl(pdma)_2\}^+$ [pdma = 1,2-phenylenebis(dimethylarsine)] centers linked to electron-deficient *fac*-$\{Re^{I}(biq)(CO)_3\}^+$ (biq = 2,2′-biquinolinyl) units. The bridging units are 4,4′-bipyridyl (4,4′-bpy), *E*-1,2-bis(4-pyridyl)ethylene (bpe), or 1,4-bis[*E*-2-(4-pyridyl)ethenyl]benzene (bpvb) ligands. A number of new monometallic precursor complexes have also been synthesized and fully characterized, primarily for purposes of comparison. The electronic absorption spectra of the bimetallic species are dominated by intense, visible $d(Ru^{II}) \rightarrow \pi^*$(4,4′-bpy/bpe/bpvb) metal-to-ligand charge-transfer (MLCT) bands and $d(Re^{I}) \rightarrow \pi^*$(biq) absorptions in the near-UV region. Cyclic voltammetric studies reveal both $Ru^{III/II}$ oxidation and ligand-based reduction processes and show no evidence for significant electronic communication between the two metal centers. Stark spectroscopic studies on the visible MLCT bands show that extending the conjugation leads to increases in the dipole moment change and the transition dipole moment, and these changes combine to afford increased static first hyperpolarizabilities, β_0, estimated by using the two-state model. Comparisons with monometallic Ru^{II} complexes reveal that methylation of the free pyridyl nitrogen leads to larger β_0 responses than does coordination of the *fac*-$\{Re^{I}(biq)(CO)_3\}^+$ center. Single-crystal X-ray structures have been determined for solvated adducts of the bimetallic complex salts *trans,fac*-$[Ru^{II}Cl(pdma)_2(\mu\text{-}L{-}L)Re^{I}(CO)_3(biq)](PF_6)_2$ (L−L = 4,4′-bpy or bpe) and also for the monometallic compounds *fac*-$[Re^{I}(biq)(CO)_3(L{-}L)]PF_6$ (L−L = 4,4′-bpy or bpe) and *trans*-$[Ru^{II}Cl(pdma)_2(L{-}L)]PF_6$ [L−L = 2,7-diazapyrene or (*E,E*)-1,4-bis(4-pyridyl)-1,3-butadiene].

Introduction

Much attention has been devoted to the study of ligand-bridged, di- and polynuclear transition metal complexes containing interacting centers. This field was given great impetus by the discovery of the Creutz−Taube ion, $[(NH_3)_5Ru(pyz)Ru(NH_3)_5]^{5+}$ (pyz = pyrazine),[1] and many other related mixed-valence complexes have been extensively investigated by using various physicochemical techniques.[2] This work has afforded a well-developed understanding of the factors determining the electronic and optical properties of ligand-bridged complexes, particularly those containing ruthenium. In addition to aspects of purely fundamental scientific interest, recent reports have shown that ligand-bridged complexes (and especially mixed-valence species) may have potential for future practical applications in the nascent fields of molecular electronics and photonics, as components of nanoscale wires/switches or in the realization of quantum computing.[3,4] Continuing investigations into such compounds are therefore valuable from several perspectives.

We have prepared and studied previously a series of homobimetallic complexes of the form *trans*-$[\{Ru^{II}Cl(pdma)_2\}_2(\mu\text{-}L{-}L)]^{2+}$ [where L−L includes pyz, fumaronitrile (fmn), 4,4′-bipyridyl (4,4′-bpy), and *E*-1,2-bis(4-pyridyl)ethylene (bpe)].[5] As expected, cyclic voltammetric measurements show that the extent of intermetallic electronic communication decreases with extension of L−L in the order pyz > fmn > 4,4′-bpy > bpe. Complexes containing the *trans*-$\{Ru^{II}Cl(pdma)_2\}^+$ center are attractive for synthetic investigations, as this five-coordinate unit is highly stable and potentially amenable to precisely controlled

* To whom correspondence should be addressed. E-mail: b.coe@manchester.ac.uk.
† University of Manchester.
‡ California Institute of Technology.
§ University of Southampton.

(1) Creutz, C.; Taube, H. *J. Am. Chem. Soc.* **1973**, *95*, 1086.
(2) (a) Creutz, C. *Prog. Inorg. Chem.* **1983**, *30*, 1. (b) Kaim, W.; Klein, A.; Glöckle, M. *Acc. Chem. Res.* **2000**, *33*, 755. (c) Demadis, K. D.; Hartshorn, C. M.; Meyer, T. J. *Chem. Rev.* **2001**, *101*, 2655. (d) Brunschwig, B. S.; Creutz, C.; Sutin, N. *Chem. Soc. Rev.* **2002**, *31*, 168. (e) Ward, M. D.; McCleverty, J. A. *J. Chem. Soc., Dalton Trans.* **2002**, 275. (f) D'Alessandro, D. M.; Keene, F. R. *Chem. Rev.* **2006**, *106*, 2270. (g) Kaim, W.; Sarkar, B. *Coord. Chem. Rev.* **2007**, *251*, 584.
(3) (a) Crutchley, R. J. *Adv. Inorg. Chem.* **1994**, *41*, 273. (b) Ward, M. D. *Chem. Soc. Rev.* **1995**, *24*, 121. (c) Otsuki, J.; Akasaka, T.; Araki, K. *Coord. Chem. Rev.* **2008**, *252*, 32.
(4) (a) Qi, H.; Sharma, S.; Li, Z.-H.; Snider, G. L.; Orlov, A. O.; Lent, C. S.; Fehlner, T. P. *J. Am. Chem. Soc.* **2003**, *125*, 15250. (b) Braun-Sand, S. B.; Wiest, O. *J. Phys. Chem. B* **2003**, *107*, 9624. (c) Jiao, J.-Y.; Long, G. J.; Rebbouh, L.; Grandjean, F.; Beatty, A. M.; Fehlner, T. P. *J. Am. Chem. Soc.* **2005**, *127*, 17819.
(5) Coe, B. J.; Hayat, S.; Beddoes, R. L.; Helliwell, M.; Jeffery, J. C.; Batten, S. R.; White, P. S. *J. Chem. Soc., Dalton Trans.* **1997**, 591.

10.1021/om800105c CCC: $40.75
Publication on Web 05/20/2008

structural extensions via chloride substitution. The present work concerns related heteronuclear bimetallic complexes in which the electron-donating *trans*-$\{Ru^{II}Cl(pdma)_2\}^+$center is connected to a *fac*-$\{Re^{I}(biq)(CO)_3\}^+$ (biq = 2,2′-biquinolinyl) electron-accepting unit via a π-conjugated bridging ligand. The primary aim of this work is to investigate the optical and electronic properties of the complexes by using a range of spectroscopic techniques and to compare the observed properties with those of monometallic reference species. A number of new mononuclear Re^{I} complexes have therefore also been synthesized, while we have reported the corresponding Ru^{II} reference compounds previously.[5–8] Transition metal complexes have recently attracted much interest as nonlinear optical (NLO) chromophores,[9] and an indirect experimental assessment of the quadratic NLO responses via electronic Stark effect (electroabsorption) spectroscopy[10] forms a component of this report.

Experimental Section

Materials and Procedures. The compound $RuCl_3 \cdot 2H_2O$ was supplied by Apollo Scientific, and pdma was obtained from Dr. G. Reid, University of Southampton. The compounds 2,7-diazapyrene (dap),[11] *trans*-$[Ru^{II}Cl(pdma)_2(NO)](PF_6)_2$,[12] *trans*-$[Ru^{II}Cl(pdma)_2(4,4'\text{-bpy})]PF_6$ (4,4′-bpy = 4,4′-bipyridyl),[5] *trans*-$[Ru^{II}Cl(pdma)_2(bpe)]PF_6$ (bpe = *E*-1,2-bis(4-pyridyl)ethylene),[5] 1,4-bis[*E*-2-(4-pyridyl)ethenyl]benzene (bpvb),[13] *trans*-$[Ru^{II}Cl(pdma)_2(bpvb)]PF_6$,[8] *E*-3-(4-pyridyl)-2-propenal,[14] 4-picolyltriphenylphosphonium chloride,[15] and *fac*-$[Re^{I}(biq)(CO)_3(MeCN)]CF_3SO_3$[16] were prepared according to published procedures. The preparation of (*E,E*)-1,4-bis(4-pyridyl)-1,3-butadiene (bpb) described below is based on a combination of literature procedures for this and related compounds.[17,18] All other reagents were obtained commercially and used as supplied. All reactions excluding the preparation of bpb were conducted in the dark, and all reactions were carried out under an argon atmosphere and in argon-purged solvents. All chromatographic purifications were performed in the dark. Products were dried at room temperature in a vacuum desiccator ($CaSO_4$) for ca. 24 h prior to characterization.

General Physical Measurements. ^{1}H NMR spectra were recorded on a Varian XL-300, a Varian Unity 400, or a Bruker Ultrashield 500 spectrometer, and all chemical shifts are quoted with respect to TMS. The midpoints are quoted for multiplet signals. Ring proton numbering and assignments for *fac*-$\{Re^{I}(biq)(CO)_3\}^+$ units are in accordance with those of Moya et al.,[19] except that the signals for the 4,4′ and 8,8′ protons are transposed; these assignments were confirmed via COSY studies with selected compounds, including **1** and **2**. Elemental analyses were performed by the Microanalytical Laboratory, University of Manchester, and UV−visible spectra were obtained by using a Hewlett-Packard 8452A diode array spectrophotometer. Infrared spectroscopy was performed on KBr disks by using a Perkin-Elmer Spectrum RX1 FT-IR spectrometer. Mass spectra were recorded by using chemical ionization on a Micromass Trio 2000 or +electrospray on a Micromass Platform II spectrometer.

Cyclic voltammetric measurements were carried out with an EG&G PAR model 283 potentiostat/galvanostat. An EG&G PAR K0264 single-compartment microcell was used with a silver/silver chloride reference electrode separated by a salt bridge from a Pt disk working electrode and Pt wire auxiliary electrode. Acetonitrile was freshly distilled (from CaH_2), and $[NBu^n_4]PF_6$, purchased from Aldrich and used as supplied, was used as the supporting electrolyte. Solutions containing ca. 10^{-3} M analyte (0.1 M electrolyte) were deaerated by purging with N_2. All $E_{1/2}$ values were calculated from $(E_{pa} + E_{pc})/2$ at a scan rate of 200 mV s^{-1}.

Synthesis of (*E,E*)-1,4-Bis(4-pyridyl)-1,3-butadiene, bpb. Sodium ethoxide (512 mg, 7.524 mmol) in ethanol (20 mL) was added dropwise to a pale yellow solution of *E*-3-(4-pyridyl)-2-propenal (200 mg, 1.502 mmol) and 4-picolyltriphenylphosphonium chloride (586 mg, 1.503 mmol) in ethanol (25 mL). After stirring at room temperature for 2 h, the brown reaction mixture was filtered and the filtrate evaporated to dryness before dissolving in 4 M hydrochloric acid. After washing with chloroform (4 × 100 mL), the pH was taken to 9 by the addition of 50% aqueous sodium hydroxide at 0 °C. The resulting oily solid was collected by filtration and then reprecipitated from ethanol/water. After standing overnight in a refrigerator, the beige solid was filtered off and washed with water. Evaporation of the filtrate gave a residue, which was precipitated from ethanol/water as above to give further product. This procedure was repeated until no further solid was collected: 74 mg, 24%. ^{1}H NMR (500 MHz, $CDCl_3$): δ 8.60 (4 H, d, J = 6.0 Hz, C_5H_4N), 7.33 (4 H, d, J = 6.0 Hz, C_5H_4N), 7.15 (2 H, d, J = 14.5 Hz, 2CH), 6.72 (2 H, d, J = 14.5 Hz, 2CH). CI-MS: m/z = 209 ($[M + H]^+$).

Synthesis of *trans*,*fac*-$[Ru^{II}Cl(pdma)_2(\mu\text{-}4,4'\text{-bpy})Re^{I}(CO)_3(biq)](PF_6)_2$ (1). A solution of *fac*-$[Re^{I}(CO)_3(biq)(MeCN)]CF_3SO_3 \cdot CHCl_3$ (108 mg, 0.129 mmol) and *trans*-$[Ru^{II}Cl(pdma)_2(4,4'\text{-bpy})]PF_6$ (65 mg, 0.064 mmol) in 2-butanone (10 mL) was heated under reflux for 5 h. Addition of aqueous NH_4PF_6 produced a red-orange precipitate, which was filtered off, washed with water, and dried. Purification was effected by sequential reprecipitations from acetone/diethyl ether, acetone/aqueous sodium tosylate, acetone/aqueous NH_4PF_6, and acetone/ether to afford a red solid: 32 mg, 30%. ^{1}H NMR (400 MHz, $(CD_3)_2CO$): δ 9.00 (2 H, d, J = 8.4 Hz, biqH$^{4,4'}$), 8.94 (2 H, d, J = 8.8 Hz, biqH$^{8,8'}$), 8.69 (2 H, d, J = 8.8 Hz, biqH$^{3,3'}$), 8.33 (2 H, d, J = 8.2 Hz, biqH$^{5,5'}$), 8.29−8.24 (6 H, C_6H_4 and biqH$^{7,7'}$), 8.02 (2 H, t, J = 7.6 Hz, biqH$^{6,6'}$), 7.80 (4 H, m, C_6H_4), 7.70 (2 H, d, J = 7.2 Hz, C_5H_4N), 7.67 (2 H, d, J = 6.8 Hz, C_5H_4N), 7.45 (2 H, d, J = 6.8 Hz, C_5H_4N), 7.30 (2 H, d, J = 6.8 Hz, C_5H_4N), 1.86 (12 H, s, 4AsMe), 1.71 (12 H, s, 4AsMe). IR ν(C≡O): 2033s, 1936br, 1918br

(6) Coe, B. J.; Beyer, T.; Jeffery, J. C.; Coles, S. J.; Gelbrich, T.; Hursthouse, M. B.; Light, M. E. *J. Chem. Soc., Dalton Trans.* **2000**, 797.
(7) Coe, B. J.; Harries, J. L.; Harris, J. A.; Brunschwig, B. S.; Coles, S. J.; Light, M. E.; Hursthouse, M. B. *Dalton Trans.* **2004**, 2935.
(8) Coe, B. J.; Harries, J. L.; Harris, J. A.; Brunschwig, B. S.; Horton, P. N.; Hursthouse, M. B. *Inorg. Chem.* **2006**, *45*, 11019.
(9) (a) Lacroix, P. G. *Eur. J. Inorg. Chem.* **2001**, 339. (b) Di Bella, S. *Chem. Soc. Rev.* **2001**, *30*, 355. (c) Goovaerts, E.; Wenseleers, W. E.; Garcia, M. H.; Cross, G. H. In *Handbook of Advanced Electronic and Photonic Materials and Devices*; Nalwa, H. S., Ed.; Academic Press: San Diego, 2001; Vol. 9, pp 127−191. (d) Coe, B. J. In *Comprehensive Coordination Chemistry II*; McCleverty, J. A., Meyer, T. J., Eds.; Elsevier Pergamon: Oxford, U.K., 2004; Vol. 9, pp 621−687. (e) Cariati, E.; Pizzotti, M.; Roberto, D.; Tessore, F.; Ugo, R. *Coord. Chem. Rev.* **2006**, *250*, 1210. (f) Coe, B. J. *Acc. Chem. Res.* **2006**, *39*, 383.
(10) (a) Liptay, W. In *Excited States*; Lim, E. C., Ed.; Academic Press: New York, 1974; Vol. 1, pp 129−229. (b) Bublitz, G. U.; Boxer, S. G. *Annu. Rev. Phys. Chem.* **1997**, *48*, 213–242.
(11) Coe, B. J.; Harris, J. A.; Asselberghs, I.; Persoons, A.; Jeffery, J. C.; Rees, L. H.; Gelbrich, T.; Hursthouse, M. B. *J. Chem. Soc., Dalton Trans.* **1999**, 3617.
(12) Douglas, P. G.; Feltham, R. D.; Metzger, H. G. *J. Am. Chem. Soc.* **1971**, *93*, 84.
(13) Amoroso, A. J.; Cargill Thompson, A. M. W.; Maher, J. P.; McCleverty, J. A.; Ward, M. D. *Inorg. Chem.* **1995**, *34*, 4828.
(14) Coe, B. J.; Jones, L. A.; Harris, J. A.; Brunschwig, B. S.; Asselberghs, I.; Clays, K.; Persoons, A.; Garín, J.; Orduna, J. *J. Am. Chem. Soc.* **2004**, *126*, 3880.
(15) Baker, B. R.; Doll, M. H. *J. Med. Chem.* **1971**, *14*, 793.
(16) Coe, B. J.; Curati, N. R. M.; Fitzgerald, E. C.; Coles, S. J.; Horton, P. N.; Light, M. E.; Hursthouse, M. B. *Organometallics* **2007**, *26*, 2318.
(17) Carsky, P.; Hünig, S.; Stemmler, I.; Scheutzow, D. *Liebigs. Ann. Chem* **1980**, 291.
(18) Coe, B. J.; Harris, J. A.; Asselberghs, I.; Wostyn, K.; Clays, K.; Persoons, A.; Brunschwig, B. S.; Coles, S. J.; Gelbrich, T.; Light, M. E.; Hursthouse, M. B.; Nakatani, K. *Adv. Funct. Mater.* **2003**, *13*, 347.
(19) Moya, S. A.; Guerrero, J.; Pastene, R.; Schmidt, R.; Sariego, R.; Sartori, R.; Sanz-Aparicio, J.; Fonseca, I.; Martínez-Ripoll, M. *Inorg. Chem.* **1994**, *33*, 2341.

cm^{-1}. Anal. Calcd (%) for $C_{51}H_{52}As_4ClF_{12}N_4O_3P_2ReRu$: C, 36.43; H, 3.12; N, 3.33. Found: C, 36.28; H, 2.99; N, 3.39. ES-MS: *m/z* = 1538 ($[M - PF_6]^+$), 864 ($[M - Re(CO)_3(biq) - 2PF_6]^+$), 709 ($[M - Re(CO)_3(biq) - 4,4'\text{-bpy} - 2PF_6]^+$), 695 ($[M - 2PF_6]^{2+}$), 525 ($[M - RuCl(pdma)_2(4,4'\text{-bpy}) - 2PF_6]^+$). Crystals suitable for X-ray diffraction studies were obtained by diffusion of diethyl ether vapor into an acetonitrile solution at room temperature.

Synthesis of *trans,fac*-[$Ru^{II}Cl(pdma)_2(\mu$-bpe)$Re^{I}(CO)_3(biq)](PF_6)_2$ (2). This compound was prepared in a fashion identical to that for **1**, by using *fac*-[$Re^{I}(CO)_3(biq)(MeCN)]CF_3SO_3 \cdot CHCl_3$ (60 mg, 0.072 mmol) and *trans*-[$Ru^{II}Cl(pdma)_2(bpe)]PF_6 \cdot 2MeCN$ (80 mg, 0.072 mmol) in place of *trans*-[$Ru^{II}Cl(pdma)_2(4,4'\text{-bpy})]PF_6$. Purification was effected by a single reprecipitation from acetone/diethyl ether to afford a red solid: 89 mg, 73%. ^1H NMR (400 MHz, $(CD_3)_2CO$): δ 9.03 (2 H, d, $J = 8.8$ Hz, biq$H^{4,4'}$), 8.97 (2 H, d, $J = 8.8$ Hz, biq$H^{8,8'}$), 8.74 (2 H, d, $J = 8.8$ Hz, biq$H^{3,3'}$), 8.35 (2 H, d, $J = 8.4$ Hz, biq$H^{5,5'}$), 8.31−8.25 (6 H, C_6H_4 and biq$H^{7,7'}$), 8.03 (2 H, t, $J = 7.6$ Hz, biq$H^{6,6'}$), 7.80 (4 H, m, C_6H_4), 7.59 (2 H, d, $J = 6.8$ Hz, C_5H_4N), 7.53 (2 H, d, $J = 6.8$ Hz, C_5H_4N), 7.27−7.18 (4 H, C_5H_4N and 2CH), 7.15 (2 H, d, $J = 6.8$ Hz, C_5H_4N), 1.86 (12 H, s, 4AsMe), 1.73 (12 H, s, 4AsMe). IR ν(C≡O): 2033s, 1935br, 1924br cm^{-1}. Anal. Calcd (%) for $C_{53}H_{54}As_4ClF_{12}N_4O_3P_2ReRu$: C, 37.28; H, 3.19; N, 3.28. Found: C, 37.28; H, 3.08; N, 2.99. ES-MS: *m/z* = 1563 ($[M - PF_6]^+$), 891 ($[M - Re(CO)_3biq - 2PF_6]^+$), 710 ($[M - Re(CO)_3(biq) - bpe - 2PF_6]^+$), 525 ($[M - RuCl(pdma)_2(bpe) - 2PF_6]^+$). Crystals suitable for X-ray diffraction studies were obtained by diffusion of diethyl ether vapor into an acetonitrile solution at room temperature.

Synthesis of *trans,fac*-[$Ru^{II}Cl(pdma)_2(\mu$-bpvb)$Re^{I}(CO)_3(biq)](PF_6)_2$ (3). This compound was prepared and purified in a fashion identical to that for **1**, by using *fac*-[$Re^{I}(CO)_3(biq)(MeCN)]CF_3SO_3 \cdot CHCl_3$ (41 mg, 0.049 mmol) and *trans*-[$Ru^{II}Cl(pdma)_2(bpvb)]PF_6 \cdot H_2O$ (60 mg, 0.052 mmol) in place of *trans*-[$Ru^{II}Cl(pdma)_2(4,4'\text{-bpy})]PF_6$. The product was obtained as an orange solid: 50 mg, 56%. ^1H NMR (500 MHz, $(CD_3)_2CO$): δ 9.09 (2 H, d, $J = 8.5$ Hz, biq$H^{4,4'}$), 9.03 (2 H, d, $J = 8.6$ Hz, biq$H^{8,8'}$), 8.81 (2 H, d, $J = 8.8$ Hz, biq$H^{3,3'}$), 8.40 (2 H, d, $J = 7.3$ Hz, biq$H^{5,5'}$), 8.36−8.31 (6 H, C_6H_4 and biq$H^{7,7'}$), 8.06 (2 H, t, $J = 7.6$ Hz, biq$H^{6,6'}$), 7.85 (4 H, m, C_6H_4), 7.59−7.51 (8 H, C_6H_4 and C_5H_4N), 7.48 (1 H, d, $J = 16.4$ Hz, CH), 7.40 (1 H, d, $J = 16.4$ Hz, CH), 7.34 (2 H, d, $J = 6.9$ Hz, C_5H_4N), 7.20 (2 H, d, $J = 6.9$ Hz, C_5H_4N), 7.15 (1 H, d, $J = 16.4$ Hz, CH), 7.10 (1 H, d, $J = 16.4$ Hz, CH), 1.90 (12 H, s, 4AsMe), 1.79 (12 H, s, 4AsMe). IR ν(C≡O): 2031s, 1920br cm^{-1}. Anal. Calcd (%) for $C_{61}H_{60}As_4ClF_{12}N_4O_3P_2ReRu$: C, 40.49; H, 3.34; N, 3.10. Found: C, 40.20; H, 3.28; N, 3.06.

Synthesis of *fac*-[$Re^{I}(biq)(CO)_3(4,4'\text{-bpy})]PF_6$ (4). A solution of *fac*-[$Re^{I}(biq)(CO)_3(MeCN)]CF_3SO_3$ (300 mg, 0.419 mmol) and 4,4′-bpy (654 mg, 4.187 mmol) was heated under reflux in methanol (100 mL) for 3 h. The volume was reduced to ca. 1 mL in vacuo, and diethyl ether was added slowly to the orange-red solution to afford an orange precipitate. The solid was filtered off, washed with diethyl ether, and dried before reprecipitation from acetone/aqueous NH_4PF_6. The crude product was loaded onto a silica gel column and eluted with dichloromethane/acetonitrile (2:1 v/v). The major orange band was collected and evaporated to dryness before drying in vacuo. Orange crystals (suitable for X-ray diffraction studies) were obtained by diffusion of diethyl ether vapor into an acetonitrile solution in the refrigerator, filtered off, and dried in vacuo: 296 mg, 85%. ^1H NMR (400 MHz, $(CD_3)_2CO$): δ 9.09 (2 H, d, $J = 8.8$ Hz, biq$H^{4,4'}$), 9.04 (2 H, d, $J = 8.8$ Hz, biq$H^{8,8'}$), 8.80 (2 H, d, $J = 8.8$ Hz, biq$H^{3,3'}$), 8.70 (2 H, d, $J = 6.0$ Hz, C_5H_4N), 8.40 (2 H, d, $J = 8.2$ Hz, biq$H^{5,5'}$), 8.33 (2 H, m, biq$H^{7,7'}$), 8.07 (2 H, m, biq$H^{6,6'}$), 7.79 (2 H, d, $J = 6.8$ Hz, C_5H_4N), 7.66 (4 H, m, $2C_5H_4N$). ν(C≡O): 2031s, 1941s, 1918s cm^{-1}. Anal. Calcd (%) for $C_{31}H_{20}F_6N_4O_3PRe$: C, 44.99; H, 2.44; N, 6.77. Found: C, 45.09; H, 2.47; N, 6.42. ES-MS: *m/z* = 683 ($[M - PF_6]^+$).

Synthesis of *fac*-[$Re^{I}(biq)(CO)_3(bpe)]PF_6$ (5). This compound was prepared and purified in a fashion identical to that for **4** by using bpe (764 mg, 4.193 mmol) in place of 4,4′-bpy. Orange crystals (suitable for X-ray diffraction studies) were obtained: 212 mg, 58%. ^1H NMR (400 MHz, $(CD_3)_2CO$): δ 9.10 (2 H, d, $J = 8.8$ Hz, biq$H^{4,4'}$), 9.03 (2 H, d, $J = 8.8$ Hz, biq$H^{8,8'}$), 8.82 (2 H, d, $J = 8.8$ Hz, biq$H^{3,3'}$), 8.64 (2 H, br s, C_5H_4N), 8.41 (2 H, d, $J = 8.0$ Hz, biq$H^{5,5'}$), 8.35 (2 H, m, biq$H^{7,7'}$), 8.08 (2 H, m, biq$H^{6,6'}$), 7.62 (4 H, m, C_5H_4N), 7.55−7.43 (4 H, 2CH and C_5H_4N). IR ν(C≡O): 2026s, 1935br, 1926s cm^{-1}. Anal. Calcd (%) for $C_{33}H_{22}F_6N_4O_3PRe \cdot H_2O$: C, 45.47; H, 2.77; N, 6.43. Found: C, 45.27; H, 2.31; N, 6.16. ES-MS: *m/z* = 709 ($[M - PF_6]^+$).

Synthesis of *fac*-[$Re^{I}(biq)(CO)_3(bpvb)]PF_6$ (6). This compound was prepared in a fashion identical to that for **4** by using *fac*-[$Re^{I}(CO)_3(biq)(MeCN)]CF_3SO_3$(150 mg, 0.209 mmol), bpvb (192 mg, 0.675 mmol) in place of 4,4′-bpy, and methanol (50 mL). The product was obtained as an orange solid: 77 mg, 38%. ^1H NMR (400 MHz, $(CD_3)_2CO$): δ 9.08 (2 H, d, $J = 8.7$ Hz, biq$H^{4,4'}$), 9.02 (2 H, d, $J = 8.7$ Hz, biq$H^{8,8'}$), 8.80 (2 H, d, $J = 8.9$ Hz, biq$H^{3,3'}$), 8.52 (2 H, d, $J = 6.4$ Hz, C_5H_4N), 8.38 (2 H, d, $J = 6.9$ Hz, biq$H^{5,5'}$), 8.32 (2 H, m, biq$H^{7,7'}$), 8.06 (2 H, m, biq$H^{6,6'}$), 7.65 (2 H, d, $J = 8.7$ Hz, C_6H_4), 7.60 (2 H, d, $J = 8.4$ Hz, C_6H_4), 7.52−7.47 (6 H, 2CH and C_5H_4N), 7.34 (2 H, d, $J = 6.9$ Hz, C_5H_4N), 7.27 (1 H, d, $J = 16.4$ Hz, CH), 7.15 (1 H, d, $J = 16.4$ Hz, CH). IR ν(C≡O): 2029s, 1918br cm^{-1}. Anal. Calcd (%) for $C_{41}H_{28}F_6N_4O_3PRe \cdot H_2O$: C, 50.57; H, 3.10; N, 5.75. Found: C, 50.48; H, 2.80; N, 5.68. ES-MS: *m/z* = 811 ($[M - PF_6]^+$).

Synthesis of *fac*-[$Re^{I}(biq)(CO)_3(MeQ^+)](PF_6)_2$ (7). A solution of **4** (80 mg, 0.097 mmol) in DMF (1.5 mL) and methyl iodide (0.5 mL) was stirred at room temperature for 32 h. The excess methyl iodide was removed in vacuo, and the addition of aqueous NH_4PF_6 gave an orange precipitate, which was filtered off, washed with water, and dried. Purification was effected by reprecipitations from acetone/diethyl ether and acetonitrile/diethyl ether: 60 mg, 63%. ^1H NMR (400 MHz, $(CD_3)_2CO$): δ 9.11 (2 H, d, $J = 6.8$ Hz, C_5H_4N), 9.06 (2 H, d, $J = 8.8$ Hz, biq$H^{4,4'}$), 9.01 (2 H, d, $J = 8.8$ Hz, biq$H^{8,8'}$), 8.75 (2 H, d, $J = 8.8$ Hz, biq$H^{3,3'}$), 8.39 (4 H, C_5H_4N and biq$H^{5,5'}$), 8.31 (2 H, m, biq$H^{7,7'}$), 8.05 (2 H, t, $J = 7.5$ Hz, biq$H^{6,6'}$), 7.92 (2 H, d, $J = 6.8$ Hz, C_5H_4N), 7.79 (2 H, d, $J = 6.8$ Hz, C_5H_4N), 4.58 (3 H, s, Me). IR ν(C≡O): 2033s, 1919br cm^{-1}. Anal. Calcd (%) for $C_{32}H_{23}F_{12}N_4O_3P_2Re$: C, 38.91; H, 2.35; N, 5.67. Found: C, 38.83; H, 1.98; N, 5.41. ES-MS: *m/z* = 843 ($[M - PF_6]^+$), 349 ($[M - 2PF_6]^{2+}$).

Synthesis of *fac*-[$Re^{I}(biq)(CO)_3(Mebpe^+)](PF_6)_2$ (8). This compound was prepared and purified in a fashion identical to **7** by using $\mathbf{5} \cdot H_2O$ (70 mg, 0.080 mmol) in place of **4** to afford an orange solid: 68 mg, 84%. ^1H NMR (500 MHz, $(CD_3)_2CO$): δ 9.10 (2 H, d, $J = 8.5$ Hz, biq$H^{4,4'}$), 9.03 (2 H, d, $J = 8.9$ Hz, biq$H^{8,8'}$), 9.00 (2 H, d, $J = 7.0$ Hz, C_5H_4N), 8.81 (2 H, d, $J = 8.5$ Hz, biq$H^{3,3'}$), 8.41 (2 H, d, $J = 8.2$ Hz, biq$H^{5,5'}$), 8.35 (2 H, m, biq$H^{7,7'}$), 8.29 (2 H, d, $J = 7.0$ Hz, C_5H_4N), 8.09 (2 H, m, biq$H^{6,6'}$), 7.82 (1 H, d, $J = 16.4$ Hz, CH), 7.71−7.55 (3 H, m, CH and C_5H_4N), 7.51 (2 H, d, $J = 6.7$ Hz, C_5H_4N), 4.54 (3 H, s, Me). IR ν(C≡O): 2026s, 1932br cm^{-1}. Anal. Calcd (%) for $C_{34}H_{25}F_{12}N_4O_3P_2Re$: C, 40.28; H, 2.49; N, 5.53. Found: C, 39.88; H, 2.29; N, 5.42. ES-MS: *m/z* = 869 ($[M - PF_6]^+$), 362 ($[M - 2PF_6]^{2+}$).

Synthesis of *fac*-[$Re^{I}(biq)(CO)_3(Mebpvb^+)](PF_6)_2$ (9). This compound was prepared and purified in a fashion identical to that for **7** by using $\mathbf{6} \cdot H_2O$ (50 mg, 0.051 mmol) in place of **4** to afford an orange solid: 40 mg, 69%. ^1H NMR (400 MHz, $(CD_3)_2CO$): δ 9.07 (2 H, d, $J = 8.8$ Hz, biq$H^{4,4'}$), 9.01 (2 H, d, $J = 8.8$ Hz, biq$H^{8,8'}$), 8.90 (2 H, d, $J = 6.8$ Hz, C_5H_4N), 8.79 (2 H, d, $J = 8.8$ Hz, biq$H^{3,3'}$), 8.38 (2 H, d, $J = 8.2$ Hz, biq$H^{5,5'}$), 8.32 (2 H, m, biq$H^{7,7'}$), 8.27 (2 H, d, $J = 7.1$ Hz, C_5H_4N), 8.05 (2 H, t, $J = 7.4$ Hz, biq$H^{6,6'}$), 7.99 (1 H, d, $J = 16.4$ Hz, CH), 7.76 (2 H, d, $J = 8.4$ Hz, C_6H_4), 7.67 (2 H, d, $J = 8.4$ Hz, C_6H_4), 7.57 (1 H, d, $J = 16.4$ Hz, CH), 7.54−7.50 (3H, CH and C_5H_4N), 7.36 (2 H, d, $J =$

6.7 Hz, C_5H_4N), 7.22 (1 H, d, $J = 16.4$ Hz, CH), 4.49 (3H, s, Me). IR ν(C≡O): 2030s, 1913br cm^{-1}. Anal. Calcd (%) for $C_{42}H_{31}F_{12}N_4O_3P_2Re \cdot H_2O$: C, 44.49; H, 2.93; N, 4.94. Found: C, 44.51; H, 2.64; N, 4.83. ES-MS: $m/z = 971$ ($[M - PF_6]^+$), 413 ($[M - 2PF_6]^{2+}$).

Synthesis of *trans*-[$Ru^{II}Cl(pdma)_2(dap)$]PF_6 (10). A solution of *trans*-[$Ru^{II}Cl(pdma)_2(NO)$]$(PF_6)_2$ (100 mg, 0.097 mmol) and NaN_3 (6.5 mg, 0.100 mmol) in acetone (5 mL) was stirred at room temperature for 2 h. 2-Butanone (10 mL) and dap (198 mg, 0.969 mmol) were added, and the acetone was removed in vacuo. The mixture was heated under reflux for 2 h and then cooled to room temperature. The reaction mixture was filtered and washed with chloroform to give a golden yellow solid: 65 mg, 62%. ^{1}H NMR (300 MHz, $(CD_3)_2SO$): δ 9.56 (2 H, s, $C_{14}H_8N_2$), 8.71 (2 H, s, $C_{14}H_8N_2$), 8.34 (2 H, d, $J = 9.0$ Hz, $C_{14}H_8N_2$), 8.25 (4 H, m, C_6H_4), 7.98 (2 H, d, $J = 9.0$ Hz, $C_{14}H_8N_2$), 7.74 (4 H, m, C_6H_4), 1.90 (12 H, s, 4AsMe), 1.60 (12 H, s, 4AsMe). Anal. Calcd (%) for $C_{34}H_{40}As_4ClF_6N_2PRu \cdot H_2O$: C, 37.96; H, 3.93; N, 2.60. Found: C, 37.88; H, 3.84; N, 2.53. ES-MS: $m/z = 915$ ($[M - PF_6]^+$). Crystals suitable for X-ray diffraction studies were obtained by diffusion of diethyl ether vapor into a dimethylsulfoxide/acetonitrile solution in a refrigerator.

Synthesis of *trans*-[$Ru^{II}Cl(pdma)_2(Medap^+)$]$(PF_6)_2$ (11). This compound was prepared in a fashion identical to **7** by using **10** · H_2O (39 mg, 0.036 mmol) in place of **4**. Purification was effected by reprecipitation from acetone/diethyl ether to afford a red solid: 32 mg; 70%. ^{1}H NMR (300 MHz, $(CD_3)_2CO$): δ 9.96 (2 H, s, $C_{14}H_8N_2$), 8.99 (2 H, s, $C_{14}H_8N_2$), 8.55 (2 H, d, $J = 9.3$ Hz, $C_{14}H_8N_2$), 8.36 (4 H, m, C_6H_4), 8.20 (2 H, d, $J = 9.0$ Hz, $C_{14}H_8N_2$), 7.87 (4 H, m, C_6H_4), 4.96 (3 H, s, $C_{14}H_8N_2$-*Me*), 1.99 (12 H, s, 4AsMe), 1.81 (12 H, s, 4AsMe). Anal. Calcd (%) for $C_{35}H_{43}As_4ClF_{12}N_2P_2Ru \cdot 2H_2O$: C, 33.53; H, 3.78; N, 2.23. Found: C, 33.47; H, 3.44; N, 2.08. ES-MS: $m/z = 1073$ ($[M - PF_6]^+$), 928 ($[M - 2PF_6]^+$), 464 ($[M - 2PF_6]^{2+}$).

Synthesis of *trans*-[$Ru^{II}Cl(pdma)_2(bpb)$]PF_6 (12). This compound was prepared in a fashion identical to **10** by using *trans*-[$Ru^{II}Cl(pdma)_2(NO)$]$(PF_6)_2$ (125 mg, 0.122 mmol) and NaN_3 (8.1 mg, 0.125 mmol) in acetone (10 mL), and bpb (117 mg, 0.562 mmol) in place of dap. After cooling to room temperature, a brown solid was removed by filtration. Addition of diethyl ether to the filtrate gave a red precipitate, which was filtered off. The solid was reprecipitated twice from acetone/diethyl ether and then from acetone/aqueous NH_4PF_6, before washing with water and drying in vacuo. Red crystals (suitable for X-ray diffraction studies) were obtained by diffusion of diethyl ether vapor into an acetonitrile solution in a refrigerator: 93 mg, 72%. ^{1}H NMR (400 MHz, $(CD_3)_2CO$): δ 8.47 (2 H, d, $J = 5.8$ Hz, C_5H_4N), 8.29 (4 H, m, C_6H_4), 7.81 (4 H, m, C_6H_4), 7.49 (2 H, d, $J = 6.2$ Hz, C_5H_4N), 7.35 (2 H, d, $J = 5.8$ Hz, C_5H_4N), 7.29−7.16 (2 H, m, 2CH), 7.10 (2 H, d, $J = 6.2$ Hz, C_5H_4N), 6.74 (1 H, d, $J = 14.4$ Hz, CH), 6.61 (1 H, d, $J = 14.6$ Hz, CH), 1.87 (12 H, s, 4AsMe), 1.75 (12 H, s, 4AsMe). Anal. Calcd (%) for $C_{34}H_{44}As_4ClF_6N_2PRu$: C, 38.46; H, 4.18; N, 2.64. Found: C, 37.95; H, 4.13; N, 2.51. ES-MS: $m/z = 918$ ($[M - PF_6]^+$).

X-Ray Crystallographic Studies. For the salts **1**, **2**, and **10**, data were collected on a Nonius Kappa CCD area-detector diffractometer controlled by the Collect software package.[20] The data were processed by Denzo[21] and corrected for absorption by using the semiempirical method employed in SADABS.[22] For the salts **4** · Et_2O, **5** · MeCN, and **12** · 1.5MeCN · 0.5Et_2O · 0.5H_2O, data were collected on a Bruker APEX CCD X-ray diffractometer. Cryocooling to 100 K was carried out by using an Oxford Cryosystems 700 Series cryostream cooler. Intensity measurements were collected using graphite-monochromated Mo Kα radiation from a sealed X-ray tube with a monocapillary collimator. Data processing was carried out by using the Bruker SAINT[23] software package, and semiempirical absorption corrections were applied by using SADABS.[22]

All of the structures were solved by direct methods and refined by full-matrix least-squares on all F_0^2 data using SHELXS-97 and SHELXL-97, respectively.[24] Generally, the non-hydrogen atoms were refined anisotropically, except where there was disorder. Hydrogen atoms were included in idealized positions using the riding model, with thermal parameters of 1.2 or 1.5 times those of the parent atoms. The crystals of **1**, **2**, and **10** contained unrefinable solvent (acetonitrile and/or diethyl ether), which was accounted for by using the SQUEEZE procedure.[25] In **1**, one of the PF_6^- anions lies on a symmetry site and another is only half-occupied. For **12** · 1.5MeCN · 0.5Et_2O · 0.5H_2O, there are two anions and cations in the asymmetric unit, together with diethyl ether and acetonitrile solvent molecules (some of the latter at 0.5 occupancy) and another solvent fragment at an occupancy of 0.5, which was defined as O (i.e., water). The second complex cation and PF_6^- anion show high thermal motion, and the atoms C59−C65 are disordered over two sites, the occupancies of which were constrained to sum to unity. The phenyl rings in this cation were constrained to be regular hexagons. The non-H atoms were refined anisotropically with restraints on those of the C atoms (except for the partially occupied atoms, which were refined isotropically). The crystal was rather weakly diffracting, and so the data were cut at 0.9 Å resolution. The *R* values for this structure are high probably because the second pair of ions was poorly ordered and also some of the solvent molecules could not be located. All other calculations for **4** · Et_2O, **5** · MeCN, and **12** · 1.5MeCN · 0.5Et_2O · 0.5H_2O were carried out by using the SHELXTL package.[26] Crystallographic data and refinement details are presented in Table 1.

Stark Spectroscopy. The Stark apparatus, experimental methods, and data analysis procedure were exactly as previously reported.[7,27,28] Butyronitrile was used as the glassing medium, for which the local field correction f_{int} is estimated as 1.33.[27,28] The Stark spectrum for each compound was measured at least twice. A two-state analysis of the MLCT transitions gives

$$\Delta\mu_{ab}^2 = \Delta\mu_{12}^2 + 4\mu_{12}^2 \quad (1)$$

where $\Delta\mu_{ab}$ is the dipole moment difference between the diabatic states, $\Delta\mu_{12}$ is the observed (adiabatic) dipole moment difference (equal to $\mu_e - \mu_g$, where μ_e and μ_g are the respective excited- and ground-state dipole moments), and μ_{12} is the transition dipole moment. Analysis of the Stark spectra in terms of the Liptay treatment[10] affords $\Delta\mu_{12}$, and the transition dipole moment μ_{12} can be determined from the oscillator strength f_{os} of the transition by

$$|\mu_{12}| = [f_{os}/(1.08 \times 10^{-5} E_{max})]^{1/2} \quad (2)$$

where E_{max} is the energy of the MLCT maximum (in wavenumbers) and μ_{12} is in Debyes. The degree of delocalization, c_b^2, and electronic coupling matrix element, H_{ab}, for the diabatic states are given by

(20) Hooft, R. *Collect. Data collection software*; Nonius BV: Delft, The Netherlands, 1998.
(21) Otwinowski, Z.; Minor, W. *Methods Enzymol.* **1997**, *276*, 307.
(22) *SADABS* (Version 2.10); Bruker AXS Inc.: Madison, WI, 2003.
(23) *SAINT* (Version 6.45); Bruker AXS Inc.: Madison, WI, 2003.
(24) Sheldrick, G. M. *SHELXL 97, Programs for Crystal Structure Analysis (Release 97-2)*; University of Göttingen: Göttingen, Germany, 1997.
(25) van der Sluis, P.; Spek, A. L. *Acta Crystallogr., Sect. A* **1990**, *46*, 194.
(26) *SHELXTL* (Version 6.10); Bruker AXS Inc.: Madison, WI, 2000.
(27) Coe, B. J.; Harris, J. A.; Brunschwig, B. S. *J. Phys. Chem. A* **2002**, *106*, 897.
(28) Shin, Y. K.; Brunschwig, B. S.; Creutz, C.; Sutin, N. *J. Phys. Chem.* **1996**, *100*, 8157.

Table 1. Crystallographic Data and Refinement Details for Complex Salts 1, 2, 4·Et$_2$O, 5·MeCN, 10, and 12·1.5MeCN·0.5Et$_2$O·0.5H$_2$O

	1	**2**	**4**·Et$_2$O	**5**·MeCN	**10**	**12**·1.5MeCN·0.5Et$_2$O·0.5H$_2$O
formula	$C_{51}H_{52}As_4ClF_{12}N_4O_3P_2ReRu$	$C_{53}H_{54}As_4ClF_{12}N_4O_3P_2ReRu$	$C_{55}H_{50}F_6N_4O_4PRe$	$C_{35}H_{25}F_6N_5O_3PRe$	$C_{34}H_{40}As_4ClF_6N_2PRu$	$C_{39}H_{54.5}As_4ClF_6N_{3.5}OPRu$
M	1681.31	1707.34	901.80	894.77	1057.85	1169.53
cryst syst	monoclinic	triclinic	triclinic	monoclinic	orthorhombic	monoclinic
space group	*C*2/*c*	*P*$\bar{1}$	*P*$\bar{1}$	*C*2/*c*	*Pnma*	*C*2/*c*
a/Å	37.219(7)	18.6640(4)	9.4515(5)	7.5141 (14)	19.6717(12)	27.355(2)
b/Å	9.3129(19)	19.5320(3)	13.6239(7)	21.864(4)	21.3529(17)	13.2876(10)
c/Å	38.793(8)	20.6710(3)	14.6204(8)	40.028(7)	11.7811(9)	57.181(4)
α/deg	90	82.645(1)	109.984(1)	90	90	90
β/deg	96.11(3)	80.929(1)	95.174(1)	94.641(3)	90	90.532(2)
γ/deg	90	77.927(1)	100.562(1)	90	90	90
U/Å^3	13370(5)	7241.6(2)	1715.32(16)	6555(2)	4948.6(6)	20784(3)
Z	8	4	2	8	4	16
T/K	120(2)	120(2)	100(2)	100(2)	120(2)	100(2)
μ/mm^{-1}	4.160	3.842	3.667	3.836	3.102	2.964
cryst size/mm	0.44 × 0.14 × 0.02	0.20 × 0.20 × 0.04	0.40 × 0.25 × 0.15	0.50 × 0.08 × 0.05	0.40 × 0.28 × 0.08	0.55 × 0.35 × 0.08
no. of reflns collected	56 647	170 644	9900	16 527	49 222	46 537
no. of indep reflns (R_{int})	13 797 (0.058)	33 179 (0.0727)	6806 (0.016)	5774 (0.069)	5797 (0.029)	14 905 (0.105)
goodness-of-fit on F^2	1.137	1.014	1.029	1.261	1.045	1.165
final R1, wR2 [$I > 2\sigma(I)$][a]	0.070, 0.176	0.049, 0.117	0.028, 0.058	0.090, 0.181	0.028, 0.080	0.122, 0.286
(all data)	0.131, 0.202	0.081, 0.127	0.024, 0.059	0.111, 0.187	0.032, 0.083	0.148, 0.305

[a] The structures were refined on F_o^2 using all data; the values of R1 are given for comparison with older refinements based on F_o with a typical threshold of $F_o > 4\sigma(F_o)$.

$$c_b^2 = \frac{1}{2}\left[1 - \left(\frac{\Delta\mu_{12}^2}{\Delta\mu_{12}^2 + 4\mu_{12}^2}\right)^{1/2}\right] \quad (3)$$

$$|H_{ab}| = \left|\frac{E_{max}(\mu_{12})}{\Delta\mu_{ab}}\right| \quad (4)$$

If the hyperpolarizability tensor β_0 has only nonzero elements along the MLCT direction, then this quantity is given by

$$\beta_0 = \frac{3\Delta\mu_{12}(\mu_{12})^2}{(E_{max})^2} \quad (5)$$

A relative error of ± 20% is estimated for the β_0 values derived from the Stark data and using eq 5, while experimental errors of ±10% are estimated for μ_{12}, $\Delta\mu_{12}$, and $\Delta\mu_{ab}$, ±15% for H_{ab}, and ± 50% for c_b^2.

Results and Discussion

Syntheses and Characterization. We have prepared the three new heterobimetallic complex salts **1**−**3** (Figure 1) in order to compare their optical and electronic properties with those of the existing monometallic compounds *trans*-[Ru^{II}Cl(pdma)$_2$-(L−L)]PF$_6$ (L−L = 4,4′-bpy **13**, bpe **14**, or bpvb **15**) and their methylated analogues **16**−**18** (Figure 2).[5−8] The new monometallic Re^I complex salts **4**−**9** were prepared to allow further comparisons. Compounds **10** and **12** were synthesized as potential precursors to heterobimetallic species containing 2,7-diazapyrene (dap) and (*E,E*)-1,4-bis(4-pyridyl)-1,3-butadiene (bpb) bridges, although unfortunately the desired products have not yet been isolated because reactions analogous to those used to prepare **1**−**3** returned only unreacted monometallic precursors. However, **10** has been N-methylated to give **11**. The N-methylated derivative of **12** (**19**) is a known complex that is synthesized via a reaction of Mebpb$^+$ with the NaN_3-treated precursor *trans*-[Ru^{II}Cl(pdma)$_2$(NO)]$^{2+}$.[8]

Reactions of **13**−**15** with *fac*-[Re^I(biq)(CO)$_3$(MeCN)]CF$_3$SO$_3$ in 2-butanone under reflux afforded the respective novel heterobimetallic species in salts **1**−**3** in moderate to good yields. The considerably higher yield of the bpe-bridged complex in **2** may be attributed to the greater basicity of its Ru^{II} precursor. Our present inability to isolate the analogous dap-bridged species may be due to a combination of lower basicity and poor solubility. The monometallic Re^I complex salts **4**−**6** were synthesized in a similar fashion; the complex in **4** has been isolated previously as its $CF_3SO_3^-$salt by Lin et al., but using different reaction conditions.[29] The monometallic Ru^{II} complex salts **10** and **12** were prepared in good yields from the NaN_3-treated precursor *trans*-[Ru^{II}Cl(pdma)$_2$(NO)]$^{2+}$. The N-methylated derivatives **7**−**9** and **11** were prepared readily via methylation of **4**−**6** and **10**, respectively, using methyl iodide in DMF. All of the new complex salts **1**−**12** were characterized by ^{1}H NMR and IR spectroscopy and CHN elemental analyses. In addition, all except for **3** also gave good +ES mass spectra.

^{1}H NMR Spectroscopy Studies. All of the new complexes display highly diagnostic ^{1}H spectra that provide some information about their electronic structures. Representative ^{1}H NMR spectra of **1**, **4**, and **7** are shown in Figure 3. Among the monometallic Re^I complexes in **4**−**9**, the resonances attributed to the biq ligands show only minor variations. However, for **4** and **5**, all of the biq signals shift slightly upfield (by 0.05−0.11

(29) Lin, R.-G.; Fu, Y.-G.; Brock, C. P.; Guarr, T. F. *Inorg. Chem.* **1992**, *31*, 4346.

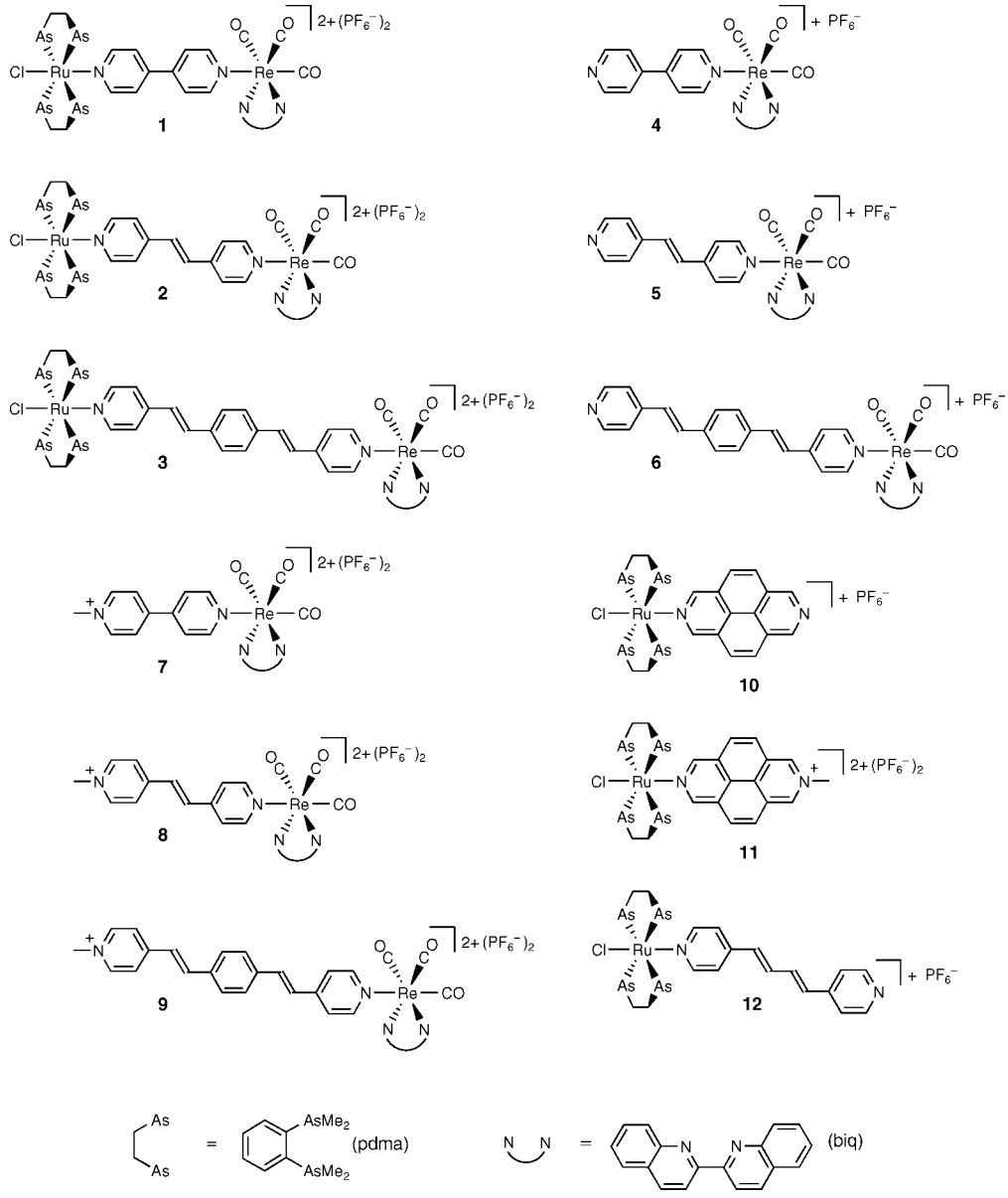

Figure 1. Structures of the new complex salts **1**−**12**.

ppm) on formation of the bimetallic complexes in **1** and **2**, respectively, but no such effect is observed in the bpvb-containing complexes **6** and **3**. These results indicate a small degree of electronic communication between the two metal centers via the relatively short 4,4′-bpy or bpe bridges in **1** and **2**, but not via the extended bpvb linkage in **3**.

Most of the signals due to the pyridyl ligands shift downfield upon methylation of the free nitrogens in **4**−**6** to give **7**−**9** (Figure 3), respectively. Although conclusive assignments of these peaks cannot be made with the available data, it can be assumed reasonably that the most downfield signal is due to the protons adjacent to the free or quaternized nitrogen atom. Upon methylation, this doublet signal shows the largest downfield shift of any of the observed resonances (ca. 0.4 ppm), consistent with the strong deshielding effect of quaternization. In the bpvb complex in **9**, this electron-withdrawing influence is communicated significantly to the phenylene ring, the doublet signals for which shift by 0.11 and 0.07 ppm, while the signals that show no significant shifts can be ascribed to the Ru^{II}-coordinated pyridyl ring. In contrast, the pyridyl ligand signals generally shift upfield on moving from **4**−**6** to the corresponding bimetallics **1**−**3**, by as much as ca. 1 ppm for the most downfield signal (Figure 3). These shifts can be attributed to the relatively strongly π-electron-donating nature of the *trans*-$\{Ru^{II}Cl(pdma)_2\}^+$ center. Smaller upfield shifts of ca. 0.1−0.2 ppm have been observed upon formation of the homobimetallic *fac*,*fac*-$[\{Re^{I}(2,2'\text{-bpy})(CO)_3\}_2(\mu\text{-}4,4'\text{-bpy})]^{2+}$ from the 2,2′-bpy analogue of **4** (in $(CD_3)_2SO$; the biq-containing homobimetallic Re^I complex was also prepared, but the data were not reported),[29] consistent with the weaker electron-donating ability of the Re^I center when compared with *trans*-$\{Ru^{II}Cl(pdma)_2\}^+$.

Electronic Spectroscopy Studies. The UV−visible absorption spectra of compounds **1**−**12** have been measured in acetonitrile, and the results are presented in Table 2, together with data for the related complex salts **13**−**19**.[5–8] Representative spectra of the bimetallic complex salts **1**−**3** are shown in Figure 4, while those of the monometallic species **7**−**9** are shown in Figure 5.

The bimetallic complexes in **1**−**3** display relatively intense, broad $d(Ru^{II}) \rightarrow \pi^*(L-L)$ (L−L = 4,4′-bpy/bpe/bpvb) MLCT bands with maxima in the region 440−462 nm (Figure 4), which are responsible for the observed orange-red colorations. Each

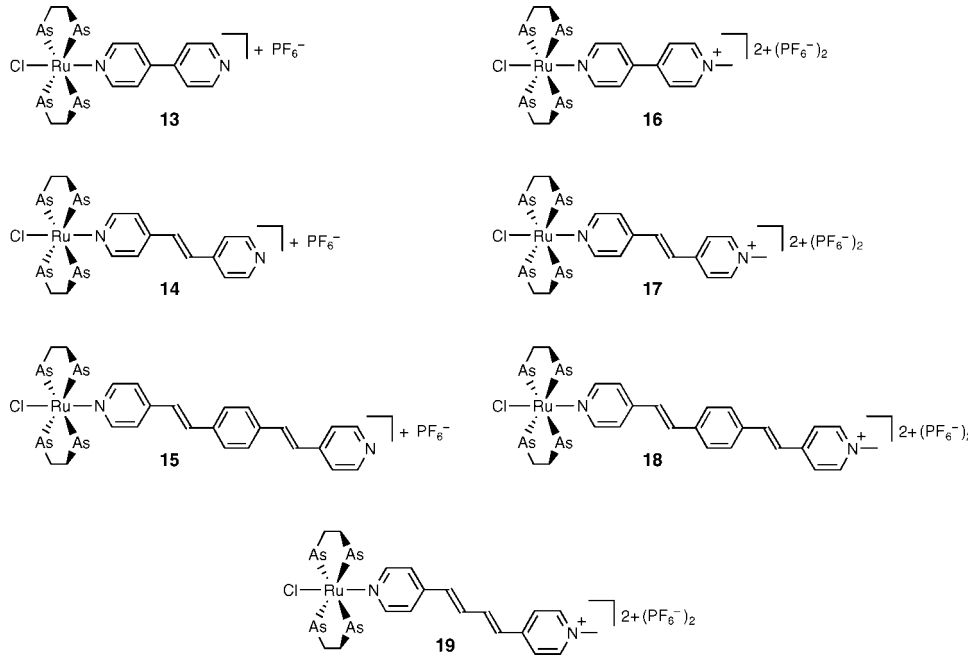

Figure 2. Structures of the known complex salts **13**−**19**.[6–8]

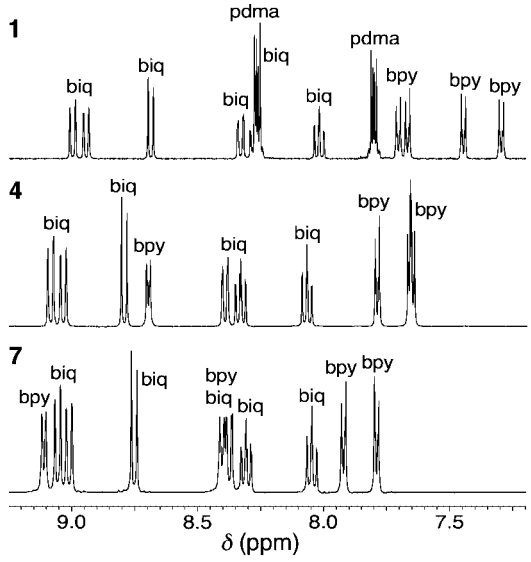

Figure 3. Aromatic regions of the ^{1}H NMR spectra of the complex salts **1**, **4**, and **7** recorded at 400 MHz in acetone-d_6 at 293 K.

of these complexes also exhibits two intense absorptions in the region 360−380 nm, which are assigned to d(Re^I) → π*(biq) MLCT transitions, and intraligand $\pi \rightarrow \pi^*$ bands are also observed to higher energies. A red-shift of the d(Ru^{II}) → π*(L−L) MLCT band is observed as the π-conjugated system is extended on moving from **1** to **2**. Further extension of L−L on moving to **3** results in a blue-shift, such that the bands for **1** and **3** occur at the same energy, although the absorption for **3** is apparently much more intense. A similar pattern is also observed in the monometallic reference series **13**−**15** and **16**−**18** (Table 2), but the energy differences on changing the pyridyl ligand are variable; E_{max} for the bpvb-containing complex in **15** is 0.1 eV lower than that of its 4,4′-bpy analogue **13**, while the reverse is true for **16** and **18**, with a difference of ca. 0.2 eV.

The increased intensity of the low-energy MLCT absorption on moving from **1** to **2** is attributable to more efficient π-orbital overlap in the extended conjugated system of the latter, and the same trend is found in the related monometallic Ru^{II} complex pairs **13**/**14** and **16**/**17**. Although further intensity increases appear to occur on moving from the bpe- to the bpvb-based chromophores, these are attributable in part to overlap with the higher energy intraligand charge-transfer (ILCT) bands. The complex in **15** shows an intense ILCT band at $\lambda_{max} = 350$ nm,[8] and it is clear that this overlaps with the d(Re^I) → π*(biq) MLCT absorptions in **3**. The low-energy tail of this combined absorption band evidently enhances the apparent intensity of the d(Ru^{II}) → π*(bpvb) transition (Figure 4). Studies with related Ru^{II} ammine complexes, which feature larger energy separations between the ILCT and MLCT bands, have shown that only relatively modest MLCT intensity increases occur on replacing a bpe with a bpvb unit.[14]

The low-energy MLCT absorptions of the reference compounds **13**−**15** undergo respective red-shifts of 0.15, 0.18, and 0.05 eV upon coordination of the *fac*-{Re^I(biq)$(CO)_3$}$^+$center to afford **1**−**3**. Such shifts are indicative of a net electron-withdrawing effect of the *fac*-{Re^I(biq)$(CO)_3$}$^+$ unit that stabilizes the L−L-based LUMO. Comparison of these MLCT bands for **1**−**3** with those of **16**−**18** reveals further red-shifts of 0.27, 0.16, and 0.03 eV, respectively. These observations indicate that the net electron-withdrawing influence of a pyridyl-coordinated *fac*-{Re^I(biq)$(CO)_3$}$^+$ unit is smaller than that of a *N*-methylpyridinium group; that is, the latter causes a greater degree of stabilization of the L−L-based LUMO. Red-shifts of the intraligand $\pi \rightarrow \pi^*$ bands are also observed on moving from **13** to **1** and along the series **14** → **2** → **17**.

The mononuclear Re^I complexes in **4**, **5**, **7**, and **8** exhibit two intense d(Re^I) → π*(biq) MLCT absorptions in the region ca. 360−380 nm. In **6** and **9**, these bands overlap with the bpvb ILCT absorptions. The positions of these high-energy MLCT bands are not affected by the nature of L−L or by coordination of the *trans*-{$Ru^{II}Cl(pdma)_2$}$^+$ center. Although **4**−**9** should also display d(Re^I) → π*(L−L) MLCT bands (that would be expected to shift to lower energies in the N-methylated species), we have found no clear evidence for these and conclude that

Table 2. UV−Visible Absorption and Electrochemical Data for Complex Salts 1−18 in Acetonitrile

compound	λ_{max}, nm (ϵ, M^{-1} cm^{-1})[a]	E_{max}, eV	assignment	$E_{1/2}$ or E, V vs Ag-AgCl (ΔE_p, mV)[b] $Ru^{III/II}$	other waves
1 *trans,fac*-$[Ru^{II}Cl(pdma)_2(\mu\text{-}4,4'\text{-bpy})Re^{I}(CO)_3(biq)](PF_6)_2$	268 (49 000)	4.63	$\pi \rightarrow \pi^*$	1.16 (60)	−0.66[c]
	308sh (17 500)	4.03	$\pi \rightarrow \pi^*$		−1.21[c]
	364 (21 300)	3.41	d → π^*(biq)		−1.48[c]
	378 (28 400)	3.28	d → π^*(biq)		
	440 (10 800)	2.82	d → π^*(4,4′-bpy)		
2 *trans,fac*-$[Ru^{II}Cl(pdma)_2(\mu\text{-bpe})Re^{I}(CO)_3(biq)](PF_6)_2$	272 (48 200)	4.56	$\pi \rightarrow \pi^*$	1.12 (80)	−1.01[c]
	302 (35 600)	4.11	$\pi \rightarrow \pi^*$(C═C)		−1.39[c]
	360 (24 200)	3.44	d → π^* (biq)		−1.78[c]
	378 (29 000)	3.28	d → π^*(biq)		
	462 (14 500)	2.68	d → π^*(bpe)		
3 *trans,fac*-$[Ru^{II}Cl(pdma)_2(\mu\text{-bpvb})Re^{I}(CO)_3(biq)](PF_6)_2$	270 (48 500)	4.59	$\pi \rightarrow \pi^*$	1.08 (70)	−0.86[c]
	366 (59 500)	3.39	d → π^* (biq)		−1.18[c]
	378 (64 300)	3.28	d → π^*(biq)		−1.50[c]
	440 (24 600)	2.82	d → π^*(bpvb)		−1.75[c]
4 *fac*-$[Re^{I}(biq)(CO)_3(4,4'\text{-bpy})]PF_6$	270 (61 300)	4.59	$\pi \rightarrow \pi^*$		−0.65 (50)[d]
	308sh (19 400)	4.03	$\pi \rightarrow \pi^*$		−1.19 (55)
	360 (22 600)	3.44	d → π^* (biq)		
	378 (32 100)	3.28	d → π^*(biq)		
5 *fac*-$[Re^{I}(biq)(CO)_3(bpe)]PF_6$	272 (56 400)	4.56	$\pi \rightarrow \pi^*$		−0.66 (50)[d]
	308sh (40 900)	4.03	$\pi \rightarrow \pi^*$ (C═C)		−1.44[c]
	360 (25 000)	3.44	d → π^* (biq)		
	378 (30 100)	3.28	d → π^*(biq)		
6 *fac*-$[Re^{I}(biq)(CO)_3(bpvb)]PF_6$	270 (41 000)	4.59	$\pi \rightarrow \pi^*$		−0.67 (50)[d]
	366sh (67 200)	3.39	d → π^* (biq)		−1.24 (50)
	378 (71 700)	3.28	d → π^*(biq)		
7 *fac*-$[Re^{I}(biq)(CO)_3(MeQ^+)](PF_6)_2$	268 (56 700)	4.63	$\pi \rightarrow \pi^*$		−0.63 (120)
	306sh (16 000)	4.05	$\pi \rightarrow \pi^*$		−0.75 (110)
	362 (21 900)	3.42	d → π^* (biq)		−1.27 (75)
	378 (28 500)	3.28	d → π^*(biq)		−1.47 (85)
8 *fac*-$[Re^{I}(biq)(CO)_3(Mebpe^+)](PF_6)_2$	272 (58 000)	4.56	$\pi \rightarrow \pi^*$		−0.65 (90)[d]
	304 (44 300)	4.08	$\pi \rightarrow \pi^*$ (C═C)		−1.17 (115)[e]
	360 (34 500)	3.44	d → π^* (biq)		−1.40 (110)[e]
	378 (36 800)	3.28	d → π^*(biq)		
9 *fac*-$[Re^{I}(biq)(CO)_3(Mebpvb^+)](PF_6)_2$	270 (55 100)	4.59	$\pi \rightarrow \pi^*$		−0.60[f]
	378 (81 000)	3.28	d → π^* (biq)		−0.69[c]
					−0.90[c]
					−1.15[f]
					−1.26[c]
10 *trans*-$[Ru^{II}Cl(pdma)_2(dap)]PF_6$	226 (63 200)	5.49	$\pi \rightarrow \pi^*$	1.15 (70)	−1.47[c]
	322 (26 700)	3.85	$\pi \rightarrow \pi^*$		
	334 (31 500)	3.71	$\pi \rightarrow \pi^*$		
	370 (9500)	3.35	$\pi \rightarrow \pi^*$		
	404 (7800)	3.07	d → π^* (dap)		
11 *trans*-$[Ru^{II}Cl(pdma)_2(Medap^+)](PF_6)_2$	240 (53 400)	5.17	$\pi \rightarrow \pi^*$	1.20 (80)	−0.80[c]
	322 (23 300)	3.85	$\pi \rightarrow \pi^*$		−1.00[c]
	338 (35 500)	3.67	$\pi \rightarrow \pi^*$		
	394 (8500)	3.15	$\pi \rightarrow \pi^*$		
	498 (7400)	2.49	d → π^* ($Medap^+$)		
12 *trans*-$[Ru^{II}Cl(pdma)_2(bpb)]PF_6$	326 (42 700)	3.80	$\pi \rightarrow \pi^*$	1.09 (70)	−1.23 (70)
	440 (18 100)	2.82	d → π^* (bpb)		−1.52 (130)
13 *trans*-$[Ru^{II}Cl(pdma)_2(4,4'\text{-bpy})]PF_6$[g]	226 (32 800)	5.49	d → π^* (4,4′-bpy)	1.14 (60)	−1.45[c]
	418 (8400)	2.97			
14 *trans*-$[Ru^{II}Cl(pdma)_2(bpe)]PF_6$[g]	228 (33 900)	5.44	$\pi \rightarrow \pi^*$	1.12 (60)	−1.29 (60)
	292 (44 300)	4.25	$\pi \rightarrow \pi^*$ (C═C)		
	434 (14 300)	2.86	d → π^* (bpe)		−1.69[c]
15 *trans*-$[Ru^{II}Cl(pdma)_2(bpvb)]PF_6$[h]	350 (51 700)	3.54	$\pi \rightarrow \pi^*$	1.07 (80)	−1.38 (100)
	432 (20 300)	2.87	d → π^* (bpvb)		
16 *trans*-$[Ru^{II}Cl(pdma)_2(MeQ^+)](PF_6)_2$[i]	486 (8300)	2.55	d → π^* (MeQ^+)	1.16 (70)	−0.72 (80)
					−1.26 (80)
17 *trans*-$[Ru^{II}Cl(pdma)_2(Mebpe^+)](PF_6)_2$[j]	316 (28 500)	3.92	$\pi \rightarrow \pi^*$	1.12 (95)	−0.77[c]
	492 (13 000)	2.52	d → π^* ($Mebpe^+$)		
18 *trans*-$[Ru^{II}Cl(pdma)_2(Mebpvb^+)](PF_6)_2$[h]	372 (34 400)	3.33	$\pi \rightarrow \pi^*$	1.08 (65)	−0.93[c]
	444 (15 600)	2.79	d → π^* ($Mebpvb^+$)		−1.61[c]
19 *trans*-$[Ru^{II}Cl(pdma)_2(Mebpb^+)](PF_6)_2$[j]	356 (37 900)	3.48	$\pi \rightarrow \pi^*$	1.11 (105)	−0.78[c]
	486 (15 700)	2.53	d → π^* ($Mebpb^+$)		

[a] Solutions ca. $3-8 \times 10^{-5}$ M. [b] Measured in solutions ca. 10^{-3} M in analyte and 0.1 M in $[NBu^n_4]PF_6$ at a Pt disk working electrode with a scan rate of 200 mV s^{-1}. Ferrocene internal reference $E_{1/2}$ = 0.45 V, ΔE_p = 60−105 mV. [c] E_{pc} for an irreversible reduction process. [d] Quasi-reversible reduction process that becomes irreversible ($i_{pa} < i_{pc}$) if scan range extended too far negative. [e] Irreversible process ($i_{pa} < i_{pc}$). [f] E_{pa} value. [g] Data taken from ref 5. [h] Data taken from ref 8. [i] Data taken from ref 6. [j] Data taken from ref 7.

they are probably obscured by the more intense d(Re^I) → π^*(biq) MLCT and ILCT absorptions. However, the spectra of **7** and **8** do display significant tails to low energies (Figure 5) that may perhaps correspond with low-intensity d(Re^I) → π^*(L−L) MLCT transitions. Other high-energy intraligand $\pi \rightarrow \pi^*$ absorptions are also observed in **4**−**9**.

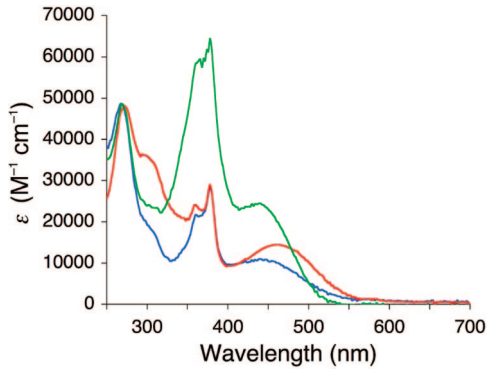

Figure 4. UV−visible absorption spectra of the heteronuclear bimetallic complex salts **1** (blue), **2** (red), and **3** (green) in acetonitrile at 293 K.

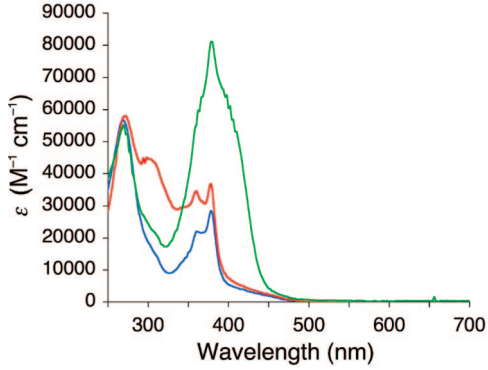

Figure 5. UV−visible absorption spectra of the monometallic complex salts **7** (blue), **8** (red), and **9** (green) in acetonitrile at 293 K.

The mononuclear Ru^{II} complexes in **10**−**12** display broad $d(Ru^{II}) \rightarrow \pi^*$(L-L) (L−L = dap, $Medap^+$, or bpb) visible MLCT bands together with intense $\pi \rightarrow \pi^*$ absorptions in the UV region. As observed in the related compounds *trans*-$[Ru^{II}(NH_3)_4(L^D)(Medap^+)](PF_6)_3$ (L^D = NH_3, pyridine, or *N*-methylimidazole),[11] **10** and **11** show four such UV bands, while **12** shows only one. As expected, methylation of the uncoordinated nitrogen in **10** to give **11** leads to a large decrease in the MLCT energy (ca. 0.6 eV), due to the increased electron-accepting ability of the *N*-methylpyridinium group. The lowest energy $\pi \rightarrow \pi^*$ band shows a concomitant red-shift of 0.2 eV. N-Methylation of **12** to give **19** causes the energies of both the MLCT and ILCT bands to decrease by ca. 0.3 eV.

Electrochemical Studies. The new complex salts **1**−**12** have been studied by cyclic voltammetry in acetonitrile, and the results are presented in Table 2, together with data for the related compounds **13**−**19**.[5–8] Representative voltammograms of **1** and **7** are shown in Figures 6 and 7.

The bimetallic complexes in **1**−**3** exhibit reversible or quasireversible $Ru^{III/II}$ oxidation waves in the region 1.08−1.16 V vs Ag-AgCl (Table 3, Figure 6). As discussed above, an ethylene unit is slightly electron donating, so the basicity of the bridging unit increases in the order 4,4′-bpy < bpe < bpvb. The coordinated Ru^{II} center therefore becomes easier to oxidize and the $Ru^{III/II}$ $E_{1/2}$ value decreases in the order **1** > **2** > **3**. Comparison of the $Ru^{III/II}$ potentials for **1**−**3** with those of the corresponding monometallic complexes in **13**−**18** reveals no significant variations, showing that the energy of the Ru-based HOMO is insensitive to coordination of the *fac*-$\{Re^I(biq-)(CO)_3\}^+$ group. These observations verify that the shifts in the low-energy MLCT bands are caused by changes in the energy of the L−L-based LUMO (see above).

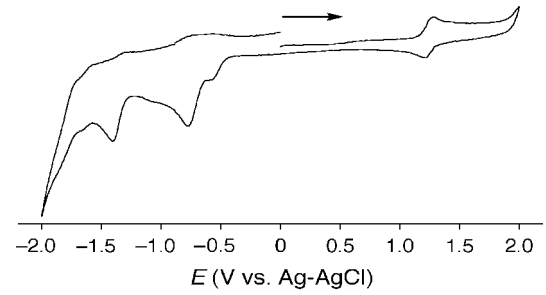

Figure 6. Representative cyclic voltammogram of the heterobimetallic complex salt **1** in acetonitrile at a scan rate of 200 mV s^{-1} (the arrow indicates the direction of the initial scan).

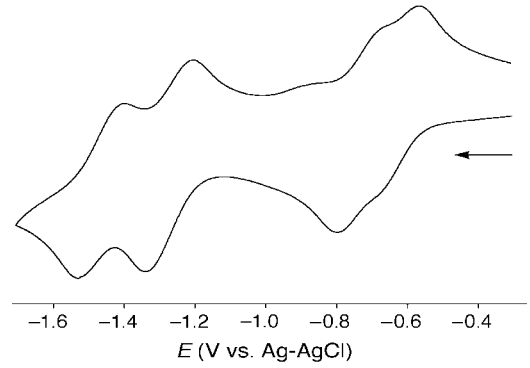

Figure 7. Representative cyclic voltammogram of the monometallic complex salt **7** in acetonitrile at a scan rate of 200 mV s^{-1} (the arrow indicates the direction of the initial scan).

Table 3. Selected Interatomic Distances (Å) and Angles (deg) for 1

Re1−C53	1.882(10)	Ru1−N21	2.111(7)
Re1−C52	1.883(11)	Ru1−As12	2.4136(13)
Re1−C51	1.913(11)	Ru1−As1	2.4080(13)
Re1−N31	2.213(8)	Ru1-A11	2.4262(11)
Re1−N32	2.188(7)	Ru1−As2	2.4087(11)
Re1−N22	2.183(8)	Ru1−Cl1	2.434(2)
C51−Re1−C53	82.8(5)	N21−Ru1−As12	93.4(2)
C51−Re1−C52	90.5(4)	N21−Ru1−As1	92.0(2)
C53−Re1−C52	89.9(5)	As12−Ru1−As1	174.55(4)
C51−Re1−N31	168.7(4)	N21−Ru1−As11	92.09(17)
C53−Re1−N31	100.8(4)	As12−Ru1−As11	85.09(4)
C52−Re1−N31	100.2(4)	As1−Ru1−As11	94.86(5)
C51−Re1−N32	101.6(4)	N21−Ru1−As2	93.43(17)
C53−Re1−N32	173.7(4)	As12−Ru1−As2	95.49(4)
C52−Re1−N32	95.0(4)	As1−Ru1−As2	84.03(4)
N31−Re1−N32	74.0(3)	As11−Ru1−As2	174.40(5)
C51−Re1−N22	89.2(3)	N21−Ru1−Cl1	176.24(19)
C53−Re1−N22	92.1(4)	As12−Ru1−Cl1	84.58(7)
C52−Re1−N22	178.4(3)	As1−Ru1- Cl1	89.99(7)
N31−Re1−N22	80.0(3)	A11-Ru1- Cl1	84.58(6)
N32−Re1−N22	83.5(3)	As2−Ru1- Cl1	89.93(6)

The complexes in **1**−**3** also exhibit a manifold of overlapping waves at negative potentials, and these ligand-based reduction processes shift slightly depending on the starting and finishing potentials selected for the measurements. Consequently, these data must be treated with caution. It is also noteworthy that the complexes in **1** and **2** exhibit apparently quasireversible reduction processes at −0.82 and −0.65 V vs Ag-AgCl, respectively, on scanning only as far as −1.0 V. However, the larger peak currents of these waves when compared with those of the corresponding $Ru^{III/II}$ waves suggests that they cannot be assigned to single redox events, but result from overlapping processes. In accordance with the previous work of Lin et al.,[29]

and with our studies with the monometallic complex salts **4**−**6** (see below), it is reasonable to assign these waves to $biq^{0/-}$ processes that overlap with reductions of the 4,4′-bpy or bpe bridging ligands.

The monometallic Re^{I} complexes in **4**−**9** show redox behavior only at negative potentials vs Ag-AgCl, which is dependent on the scan range in a similar manner to that of **1**−**3**. For **4**−**6**, the first reduction process (attributable to $biq^{0/-}$) is quasireversible. When this process is scanned in isolation, it appears almost reversible, but scanning too far to negative potentials introduces irreversibility. The complexes in **4**−**6** also exhibit a second well-defined reduction process, probably $biq^{-/2-}$ in nature, which is quasireversible for **4** and **6**, but irreversible for **5**. Poorly resolved features in between these two biq-based waves are also observed that are presumably attributable to the 4,4′-bpy/bpe/bpvb ligands.

The complex in **7** exhibits a total of four quasireversible reduction processes, the first two of which are closely overlapped (Figure 7). Comparison with **4** suggests that the second and fourth of these waves at −0.75 and −1.47 V vs Ag-AgCl may be assigned to $MeQ^{+/0}$ and $MeQ^{0/-}$ processes, respectively (with the $biq^{0/-}$ wave being almost unshifted, while the $biq^{-/2-}$ wave shifts by −80 mV). Previous studies on Ru^{II} complexes of the MeQ^{+} ligand, including that in **16**,[6] and also various ammine-containing species[14] have revealed two often reversible reduction processes. When compared with its precursor **5**, the complex in **8** displays an additional irreversible reduction process that can be attributed to reduction of the $Mebpe^{+}$ ligand. In contrast, the electrochemical behavior of **9** is disappointingly complicated, with no evidence for any even remotely reversible processes.

The new mononuclear Ru^{II} complexes in **10**−**12** show reversible or quasireversible $Ru^{III/II}$ oxidation waves, together with quasireversible or irreversible L−L-based reductions. These data confirm that the red-shifting of the MLCT absorption band upon methylation of **10** to form **11** (see above) can largely be attributed to a marked stabilization of the dap-based LUMO, although an increase of 50 mV in the $Ru^{III/II}$ potential shows a small concomitant stabilization of the Ru-based HOMO. A similar pattern of redox behavior is observed when comparing the pair **12** and **19**.

Crystallographic Studies. Single-crystal X-ray structures have been obtained for the complex salts **1**, **2**, **4**·Et_2O, **5**·MeCN, **10**, and **12**·1.5MeCN·0.5Et_2O·0.5H_2O. The crystals of **1**, **2**, and **10** also contained acetonitrile and/or diethyl ether solvent molecules, but these could not be refined and were therefore accounted for by using the SQUEEZE procedure.[25] Representations of the molecular structures are shown in Figures 8–13, and selected interatomic distances and angles are presented in Tables 3–7.

The molecular structures of all of the complexes are as indicated by ^{1}H NMR spectroscopy and show geometric parameters that are consistent with data reported previously for *trans*-$\{Ru^{II}Cl(pdma)_2\}^{+}$ and *fac*-$\{Re^{I}(biq)(CO)_3\}^{+}$ compounds.[5–7,16] In particular, the structure of **1** is similar to that of its 2,2′-bipyridyl analogue.[30] Once again, we observe that the biq ligands are bowed about their central C−C bonds and strongly tilted out of the equatorial plane defined by the Re^{I} ion and the trans carbonyl ligands, toward the pyridyl ligand.[16] The dihedral angles between the pyridyl rings in salts **1** and **2** are 7.4° and 20.9/19.0° and 15.8° (two independent cations, the first disordered over two sites), respectively. The corresponding respective angles in the monometallic precursors **13** and **14** are 10.3° and 5.2°,[6,7] while those for the complexes in **4**·Et_2O, **5**·MeCN, and **12**·1.5MeCN·0.5Et_2O·0.5H_2O are 6.1°, 4.6°, and 7.0/6.2° (ordered/disordered cations), respectively. The complex in

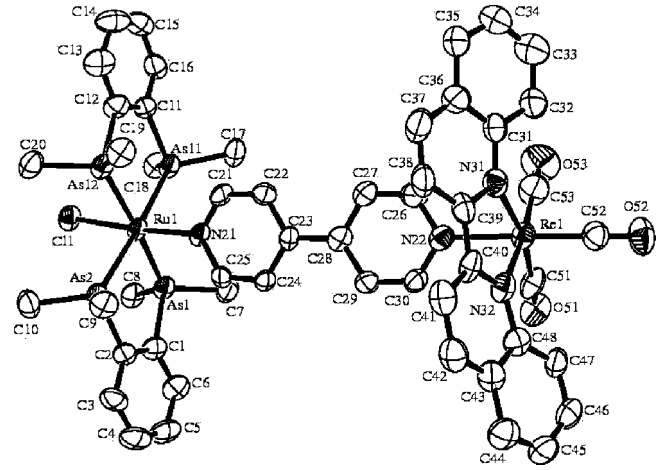

Figure 8. Representation of the molecular structure of the complex cation in the salt **1** (50% probability ellipsoids).

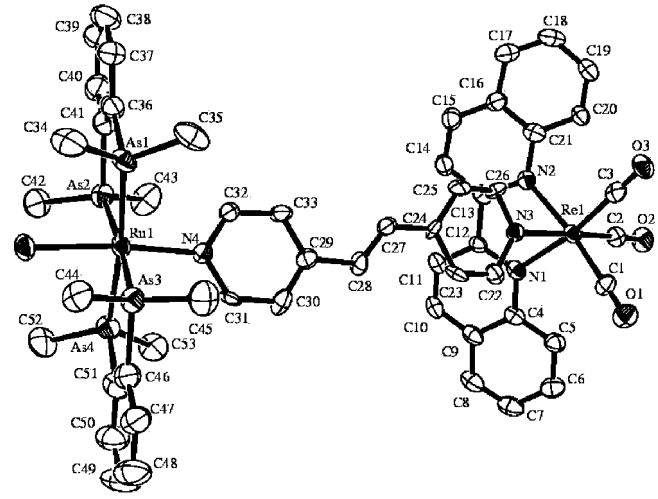

Figure 9. Representation of the molecular structure of one of the two independent complex cations in the salt **2** (50% probability ellipsoids).

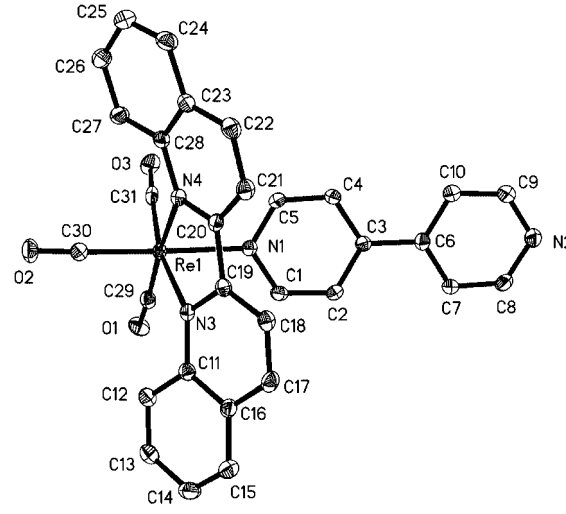

Figure 10. Representation of the molecular structure of the complex cation in the salt **4**·Et_2O (50% probability ellipsoids).

(30) Coe, B. J.; McDonald, C. I.; Coles, S. J.; Hursthouse, M. B. *Acta Crystallogr., Sect. C* **2000**, *56*, 963.

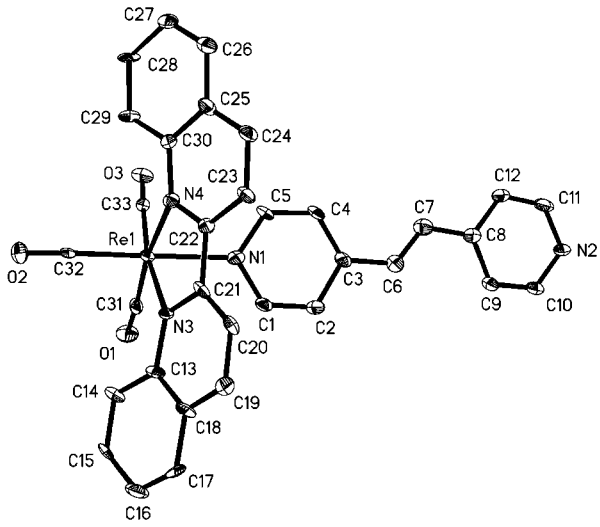

Figure 11. Representation of the molecular structure of the complex cation in the salt **5**·MeCN (50% probability ellipsoids).

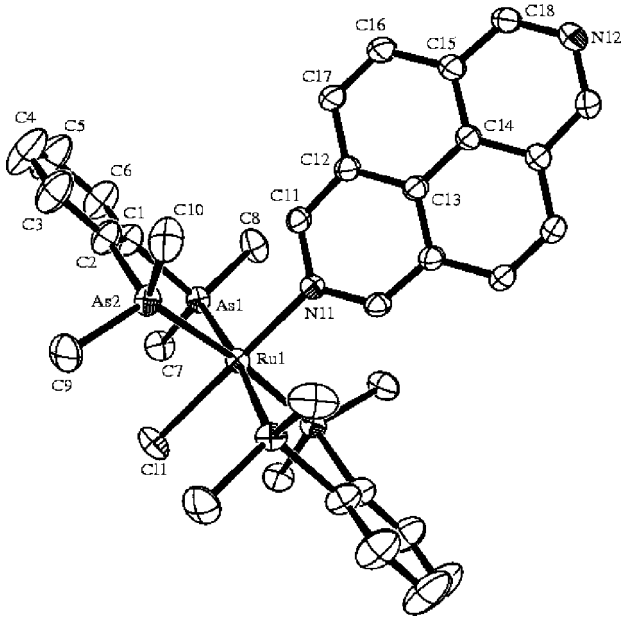

Figure 12. Representation of the molecular structure of the complex cation in the salt **10** (50% probability ellipsoids).

trans,fac-[$Ru^{II}Cl(pdma)_2(\mu$-4,4′-bpy)$Re^{I}(CO)_3$(2,2′-bpy)]$(PF_6)_2$·$2Me_2CO$ shows a dihedral angle of 13.9° within the 4,4′-bpy bridge.[30] Our previous studies with related complexes have established that such dihedral angles are primarily attributable to crystal packing factors and give no indication of the strength of π-electronic coupling within the pyridyl ligands.[6]

Stark Spectroscopic Studies. In order to provide further insights into their molecular electronic properties, including NLO responses, the bimetallic compounds **1**−**3** have been studied by electronic Stark effect (electroabsorption) spectroscopy in butyronitrile glasses at 77 K. The results are presented in Table 8, together with data reported previously for the monometallic Ru^{II} compounds **16**−**18**.[7,8] For **3**, satisfactory data could only be obtained for the low-energy d(Ru^{II}) → π*(bpvb) MLCT band and not the higher energy d(Re^{I}) → π*(biq) MLCT bands, because the area below 420 nm has a very weak Stark spectrum and many absorption peaks. Consequently, the corresponding transitions possess relatively small $\Delta\mu_{12}$ values and are not expected to contribute significantly to the overall NLO response. In a similar manner, only the d(Ru^{II}) → π*(4,4′-bpy/bpe) MLCT bands were studied for compounds **1** and **2**. Compounds **7**−**9** were also subjected to Stark spectroscopy.

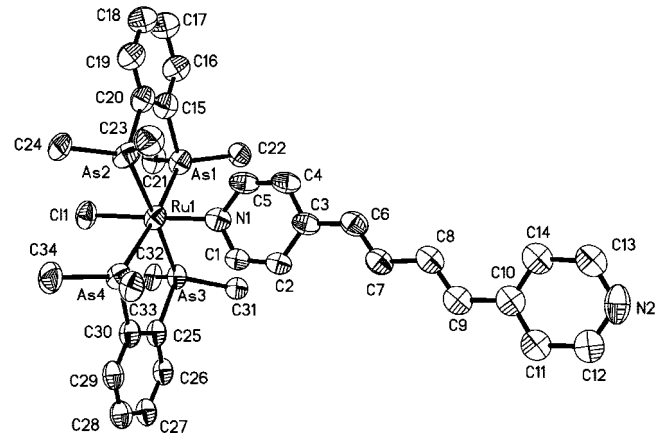

Figure 13. Representation of the molecular structure of the ordered complex cation in the salt **12**·1.5MeCN·0.5Et_2O·0.5H_2O (50% probability ellipsoids).

Table 4. Selected Interatomic Distances (Å) and Angles (deg) for 2

Re1−C1	1.925(5)	Ru1−N4	2.118(10)
Re1−C2	1.923(6)	Ru1−As4	2.4157(7)
Re1−C3	1.929(6)	Ru1−As1	2.4239(7)
Re1−N1	2.198(4)	Ru1-A3	2.4136(7)
Re1−N2	2.191(4)	Ru1−As2	2.4204(7)
Re1−N3	2.216(11)	Ru1−Cl1	2.4322(15)
C3−Re1−C1	85.5(2)	N4−Ru1−As4	89.3(9)
C3−Re1−C2	89.4(2)	N4−Ru1−As1	96.7(9)
C1−Re1−C2	89.6(2)	As4−Ru1−As1	174.02(3)
C3−Re1−N1	170.7(2)	N4−Ru1−As3	87.6(8)
C1−Re1−N1	102.2(2)	As4−Ru1−As3	85.17(2)
C2−Re1−N1	95.67(19)	As1−Ru1−As3	94.93(2)
C3−Re1−N2	97.44(19)	N4−Ru1−As2	97.0(8)
C1−Re1−N2	171.3(2)	As4−Ru1−As2	94.82(3)
C2−Re1−N2	98.63(19)	As1−Ru1−As2	84.60(2)
N1−Re1−N2	74.12(16)	As3−Ru1−As2	175.43(3)
C3−Re1−N3	95(2)	N4−Ru1−Cl1	173.8(4)
C1−Re1−N3	91.7(17)	As4−Ru1−Cl1	86.80(4)
C2−Re1−N3	176(2)	As1−Ru1−Cl1	87.23(4)
N1−Re1−N3	80(2)	A3−Ru1-Cl1	87.26(4)
N2−Re1−N3	79.9(18)	As2−Ru1−Cl1	88.17(4)

Table 5. Selected Interatomic Distances (Å) and Angles (deg) for 4·Et_2O and 5·MeCN

	4·Et_2O	**5**·MeCN
Re−N(biq)	2.204(2)	2.206(12)
Re−N(biq)	2.194(2)	2.184(12)
Re−N(L−L)[a]	2.203(2)	2.192(12)
Re−C(trans-biq)	1.920(3)	1.924(14)
Re−C(trans-biq)	1.922(3)	1.916(15)
Re−C(trans-L-L)	1.928(3)	1.922(14)
N(biq)−Re−N(biq)	74.25(8)	74.3(4)
N(biq)−Re−N(L−L)	80.38(8)	81.8(4)
N(biq)−Re−N(L−L)	83.79(8)	83.5(5)
N(biq)−Re−C(trans-biq)	168.00(10)	172.5(5)
N(biq)−Re−C(trans-biq)	100.51(10)	99.1(5)
N(biq)−Re−C(trans-biq)	174.60(10)	170.3(5)
N(biq)−Re−C(trans-biq)	99.12(10)	100.4(5)
N(biq)−Re−C(trans-L-L)	100.35(10)	97.2(5)
N(biq)−Re−C(trans-L-L)	94.81(10)	96.6(5)
N(L-L)−Re−N(trans-biq)	89.05(10)	92.3(5)
N(L-L)−Re−N(trans-biq)	94.10(10)	88.6(5)
N(L-L)−Re−N(trans-L-L)	178.20(9)	178.9(5)
C(trans-biq)−Re−N(trans-biq)	85.80(12)	85.4(6)
C(trans-biq)−Re−N(trans-L-L)	90.05(11)	88.7(6)
C(trans-biq)−Re−N(trans-L-L)	87.39(12)	91.2(6)

[a] L−L = 4,4′-bpy (**4**·Et_2O), bpe (**5**·MeCN).

Table 6. Selected Interatomic Distances (Å) and Angles (deg) for 10

Ru1−As1	2.4161(3)	Ru1−Cl1	2.4173(9)
Ru1−As2	2.4142(3)	Ru1−N11	2.109(3)
As1−Ru1−As2	84.722(10)	As2−Ru1−Cl1	86.844(17)
As1−Ru1−Cl1	86.728(17)	As2−Ru1−N11	93.62(5)
As1−Ru1−N11	92.81(5)	Cl1−Ru1−N11	179.31(7)

Table 7. Selected Interatomic Distances (Å) and Angles (deg) for 12

Ru2−As5	2.417(3)	Ru2−As7	2.414(2)
Ru2−As6	2.412(2)	Ru2−Cl2	2.435(5)
Ru2−As8	2.403(3)	Ru2−N3	2.118(14)
As5−Ru2−As6	84.70(8)	As6−Ru2−N3	92.4(4)
As5−Ru2−As8	174.36(10)	As8−Ru2−As7	84.58(9)
As5−Ru2−As7	95.84(9)	As8−Ru2−Cl2	87.89(15)
As5−Ru2−Cl2	86.50(15)	As8−Ru2−N3	93.5(4)
As5−Ru2−N3	92.2(4)	As7−Ru2−Cl2	88.86(14)
As6−Ru2−As8	94.50(8)	As7−Ru2−N3	91.5(4)
As6−Ru2−As7	176.03(10)	Cl2−Ru2−N3	178.6(4)
As6−Ru2−Cl2	87.25(14)		

However, as predicted from the electronic spectroscopy studies (see above), the presence of multiple overlapped MLCT bands means that the results obtained are of limited value and will not be considered here.

The $d(Ru^{II}) \rightarrow \pi^*(L-L)$ MLCT bands of **1**−**3** show red-shifts on moving from acetonitrile solution to butyronitrile glass, an effect that is also observed with the monometallic reference compounds **16**−**18** and other related Ru^{II} salts.[7,8,14,27] However, the extent of this shifting varies over a range of 0.02−0.16 eV. On moving from **1** to **2**, E_{max} decreases, while μ_{12} and $\Delta\mu_{12}$ both increase. These effects are all predictable on the basis of the normal behavior of such aromatic chromophores and correlate with an approximately 2-fold increase in β_0 upon extension of the conjugated bridge. Further increases in μ_{12} and $\Delta\mu_{12}$ are observed on moving from **2** to **3**, and E_{max} also increases. Again, these changes parallel those observed previously in related Ru^{II} ammine complexes[14] and also purely organic systems in which the incorporation of *E*,*E*-1,4-bis(ethenyl)phenylene bridges has been proposed as a strategy for increasing optical transparency and stability while maintaining relatively large NLO responses.[31] The apparent slight increase in β_0 on moving from **2** to **3** is within the experimental error (±20%). As expected, $\Delta\mu_{ab}$ also increases as the length of the bridge increases, and the values for $\Delta\mu_{ab}$ are larger than those of $\Delta\mu_{12}$ in each case.

As noted above for acetonitrile solutions, the MLCT bands of the bimetallic complexes **1**−**3** are blue-shifted when compared with those of their monometallic Ru^{II} analogues when measured in butyronitrile at 77 K. The largest blue-shift occurs on moving from **16** to **1** (0.23 eV), and this shift becomes progressively smaller on moving from **17** to **2** (0.12 eV) and from **18** to **3** (0.07 eV). Hence, the effect on the MLCT energy gap of changing the structure of the acceptor fragment decreases as the bridge is extended. In contrast with the new bimetallics, the μ_{12} values for the monometallic species show no clear dependence on the conjugation length, but μ_{12} is consistently slightly larger for the latter chromophores. The greatest observed difference in μ_{12} is between salts **1** and **16** (2 D). The $\Delta\mu_{12}$ values also increase with conjugation length in the monometallic series and are larger in the bimetallics, although those for salts **1** and **16** are very similar. In each instance, the values of β_0 derived by using the two-state model are larger for the monometallic reference complexes. The approximately 2-fold decrease in β_0 on moving from **16** to **1** is attributable to an increase in E_{max} and a decrease in μ_{12}, together with a minimal change in $\Delta\mu_{12}$. In contrast, the pairs **2**/**17** and **3**/**18** have similar β_0 values (within experimental error) due to the more substantially increased $\Delta\mu_{12}$ values for the bimetallic complexes.

Of the bimetallic complexes, **1** has the largest values of both c_b^2 and H_{ab}, indicating that this chromophore has the largest degree of electron donor−acceptor orbital mixing. These observations reflect the trends found in the monometallic reference series and in previous studies[14] and are attributable to the fact that **1** contains the shortest π-conjugated bridge. It should be noted that the maximum value that can be obtained for c_b^2 is 0.5, which corresponds with complete delocalization of the orbitals involved in the electronic transition.

Although the difference in β_0 between the pairs **2**/**17** and **3**/**18** is within the experimental error, the presence of a consistent trend provides reasonably convincing evidence that the monometallics exhibit the larger NLO responses. This observation is primarily attributable to the increased MLCT energies for the bimetallic complexes, consistent with the *N*-methylpyridinium group being a better electron acceptor than the *fac*-$\{Re^{I}(biq-)(CO)_3\}^+$ unit. The larger μ_{12} values for the monometallics are another contributing factor. The values of β_0 estimated for **1**−**3** are relatively large and similar to those determined previously for heterobimetallic complexes; hyper-Rayleigh scattering (HRS) measurements with a number of complexes with electron-rich Ru^{II} σ-acetylide centers connected to $M^0(CO)_5$ (M = Cr or W) acceptors gave β_0 values of up to 150×10^{-30} esu.[32] However, considerably larger responses, in some cases exceeding 500×10^{-30} esu, have been determined for other mononuclear Ru^{II}-based chromophores, including ammine species.[14] Other NLO investigations with heterobimetallic complexes have mostly followed early reports of compounds featuring a ferrocenyl (Fc) electron donor group.[33] HRS studies have been carried out on Fc complexes with metal pentacarbonyl acceptors, including $Re^{I}(CO)_5$,[34] but it is unfortunately not possible to derive meaningful β_0 values for such complexes due to inapplicability of the two-state model.

Conclusion

We have synthesized three new heterobimetallic complexes in which the *trans*-$\{RuCl(pdma)_2\}^+$ center is linked to a *fac*-$\{Re^{I}(biq)(CO)_3\}^+$ unit via a 4,4′-bpy, bpe, or bpvb bridging ligand, together with a number of monometallic Re^{I} or Ru^{II} reference complexes. The UV−visible absorption spectra of the bimetallic species display both $d(Re^{I}) \rightarrow \pi^*(biq)$ and $d(Ru^{II}) \rightarrow \pi^*(L-L)$ (L−L = 4,4′-bpy/bpe/bpvb) MLCT bands. The energies of the latter are decreased when compared with those of the corresponding monometallic Ru^{II} complexes, but higher than those of the related species with electron-withdrawing

(31) (a) Alain, V.; Rédoglia, S.; Blanchard-Desce, M.; Lebus, S.; Lukaszuk, K.; Wortmann, R.; Gubler, U.; Bosshard, C.; Günter, P. *Chem. Phys.* **1999**, *245*, 51. (b) Luo, J.-D.; Hua, J.-L.; Qin, J.-G.; Cheng, J.-Q.; Shen, Y.-C.; Lu, Z.-H.; Wang, P.; Ye, C. *Chem. Commun.* **2001**, 171.

(32) (a) Houbrechts, S.; Clays, K.; Persoons, A.; Cadierno, V.; Gamasa, M. P.; Gimeno, J. *Organometallics* **1996**, *15*, 5266. (b) Cadierno, V.; Conejero, S.; Gamasa, M. P.; Gimeno, J.; Asselberghs, I.; Houbrechts, S.; Clays, K.; Persoons, A.; Borge, J.; García-Granda, S. *Organometallics* **1999**, *18*, 582.

(33) (a) Coe, B. J.; Jones, C. J.; McCleverty, J. A.; Bloor, D.; Kolinsky, P. V.; Jones, R. J. *J. Chem. Soc., Chem. Commun.* **1989**, 1485. (b) Coe, B. J.; Foulon, J.-D.; Hamor, T. A.; Jones, C. J.; McCleverty, J. A.; Bloor, D.; Cross, G. H.; Axon, T. L. *J. Chem. Soc., Dalton Trans.* **1994**, 3427. (c) Coe, B. J.; Jones, C. J.; McCleverty, J. A.; Bloor, D.; Kolinsky, P. V.; Jones, R. J. *Polyhedron* **1994**, *13*, 2107. (d) Coe, B. J.; Hamor, T. A.; Jones, C. J.; McCleverty, J. A.; Bloor, D.; Cross, G. H.; Axon, T. L. *J. Chem. Soc., Dalton Trans.* **1995**, 673.

(34) (a) Lee, I. S.; Lee, S. S.; Cheung, Y. K.; Kim, D.; Song, N. W. *Inorg. Chim. Acta* **1998**, *279*, 243. (b) Mata, J.; Uriel, S.; Peris, E.; Llusar, R.; Houbrechts, S.; Persoons, A. *J. Organomet. Chem.* **1998**, *562*, 197.

Table 8. Visible MLCT Absorption and Stark Spectroscopic Data for Complex Salts 1−3 and 16−18

salt	λ_{max},[a] nm	λ_{max},[b] nm	E_{max},[b] eV	f_{os},[b]	μ_{12},[c] D	$\Delta\mu_{12}$,[d] D	$\Delta\mu_{ab}$,[e] D	c_b^2,[f]	H_{ab},[g] cm^{-1}	β_0,[h] 10^{-30} esu
1	440	449	2.76	0.22	4.6	14.5	17.2	0.08	6000	47
2	462	491	2.53	0.30	5.6	20.1	23.0	0.06	4900	114
3	440	459	2.70	0.36	6.0	22.8	24.6	0.06	5300	122
16[i]	486	491	2.53	0.41	6.6	14.3	19.4	0.13	6900	113
17[i]	492	515	2.41	0.33	6.0	16.9	20.7	0.09	5600	123
18[j]	444	471	2.63	0.4	6.4	18.8	22.8	0.09	6000	131

[a] Measured in acetonitrile solutions at 293 K. [b] Measured in butyronitrile glasses at 77 K. [c] Calculated from eq 2. [d] Calculated from $f_{int}\Delta\mu_{12}$ by using $f_{in\ t} = 1.33$. [e] Calculated from eq 1. [f] Calculated from eq 3. [g] Calculated from eq 4. [h] Calculated from eq 5. [i] Data taken from ref 7. [j] Data taken from ref 8.

N-methylpyridinium groups. ^{1}H NMR data for the biq ligands indicate a small degree of electronic communication between the two metal centers via the relatively short 4,4′-bpy or bpe bridges, but not via the bpvb linkage. However, cyclic voltammetric studies provide no clear evidence for intermetallic electronic communication. Stark spectroscopic studies show that extending the conjugation leads to increases in $\Delta\mu_{12}$ and μ_{12} and in the β_0 values estimated by using the two-state model. Comparisons with monometallic Ru^{II} reference complexes reveal that methylation of the free pyridyl nitrogen leads to larger NLO responses than does coordination of the *fac*-$\{Re^{I}(biq)(CO)_3\}^+$ center. This outcome can be attributed to the fact that the latter group is a weaker net electron acceptor; although the Re^{I}-based moiety is a strong Lewis acid, it also behaves as a π-donor, and this offsets its electron-withdrawing effect. In contrast, a *N*-methylpyridinium group possesses no such ambivalent electronic behavior. Because the available data are presently somewhat limited, further studies with species containing other bridging ligands will allow firmer conclusions to be drawn.

Acknowledgment. We thank the EPSRC for support (a Ph.D. studentship for E.C.F.).

Supporting Information Available: X-ray crystallographic data in CIF format. This material is available free of charge via the Internet at http://pubs.acs.org.

OM800105C